Experiments at Extreme States of Matter - High Energy Density Physics at the National Ignition Facility

Gail Glendinning
Lawrence Livermore National Laboratory

Fri., Oct. 31, 2008, 12:45 PM

Today: *Pre-colloquium* talk by
David Cohen
Swarthmore College

Experiments at Extreme States of Matter - High Energy Density Physics at the National Ignition Facility

The *National Ignition Facility* is a 1.8 Megajoule laser currently under construction at the Lawrence Livermore National Laboratory. When complete, it will be used to research fundamental questions about matter in extreme states. In 2003, the National Research Council published a report titled *Frontiers in High Energy Density Physics: The X-Games of Contemporary Science*. Their conclusion was that experimental facilities such as the NIF, Sandia's Z machine, and SLAC (among others) are now capable of reaching regimes of high energy density allowing unprecedented insight into the behavior of matter under extreme conditions. We describe in this presentation experiments planned for the NIF and current experiments at existing facilities addressing some of the questions posed in this report:

- How does matter behave under conditions of extreme temperature, pressure, and density?
- Can the transition to turbulence, and the turbulent state, in high energy density systems be understood experimentally and theoretically?
- Will measurements of the equation of state and opacity of materials at high temperatures and pressures change models of stellar and planetary structure?

Outline

HEDP and large lasers

Inertial Confinement Fusion

Hydrodynamics, instabilities

Equation of state

Opacities

High Energy Density Physics

Def'n: energy/volume > 10^{12} ergs cm^{-3}

> 10^{11} J m^{-3}

energy/volume = nkT

number density (cm^{-3})

Boltzmann's constant X temperature (ergs)

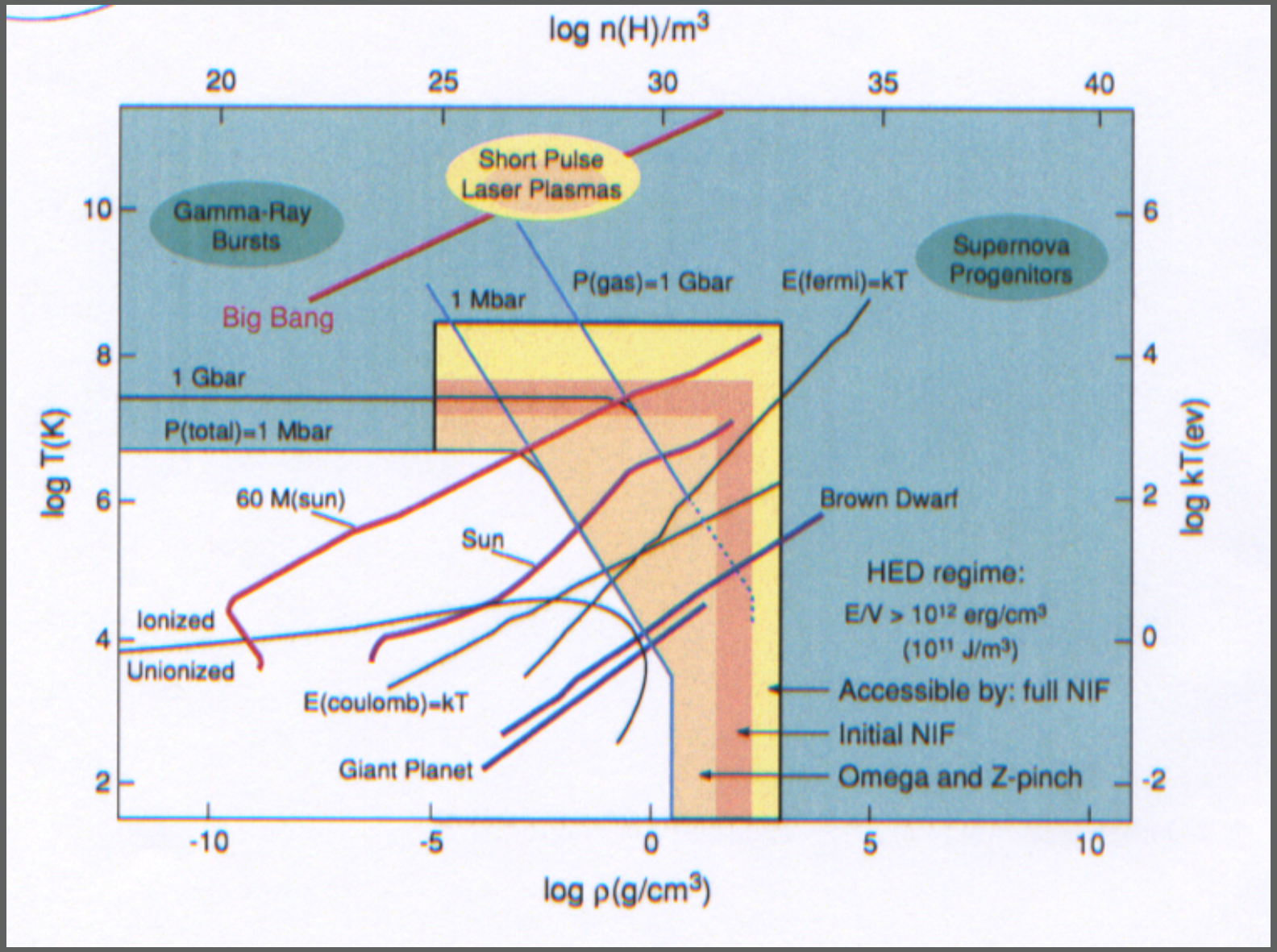
log n(H)/m3
20
25
30
35
40
Short Pulse
Laser Plasmas
Gamma-Ray
Bursts
Supernova
Progenitors
P(gas)=1 Gbar
E(fermi)=kT
1 Mbar
Big Bang
1 Gbar
P(total)=1 Mbar
60 M(sun)
Sun
Brown Dwarf
HED regime:
E/V > 10^12 erg/cm^3
(10^11 J/m^3)
Ionized
Unionized
E(coulomb)=kT
Accessible by: full NIF
Initial NIF
Omega and Z-pinch
Giant Planet
log T(K)
log kT(ev)
10
8
6
4
2
6
4
2
0
-2
-10
-5
0
5
10
log ρ(g/cm3)

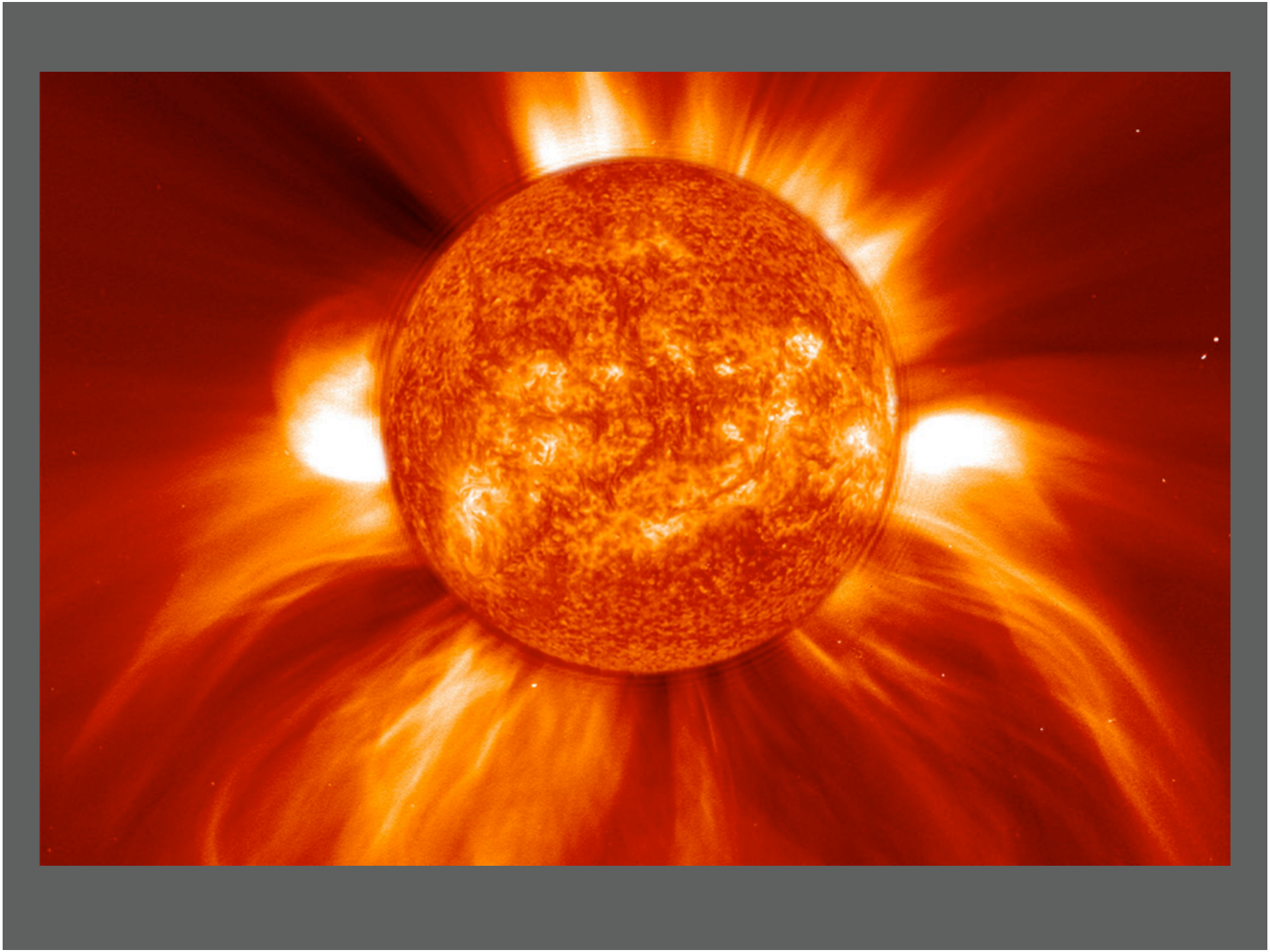

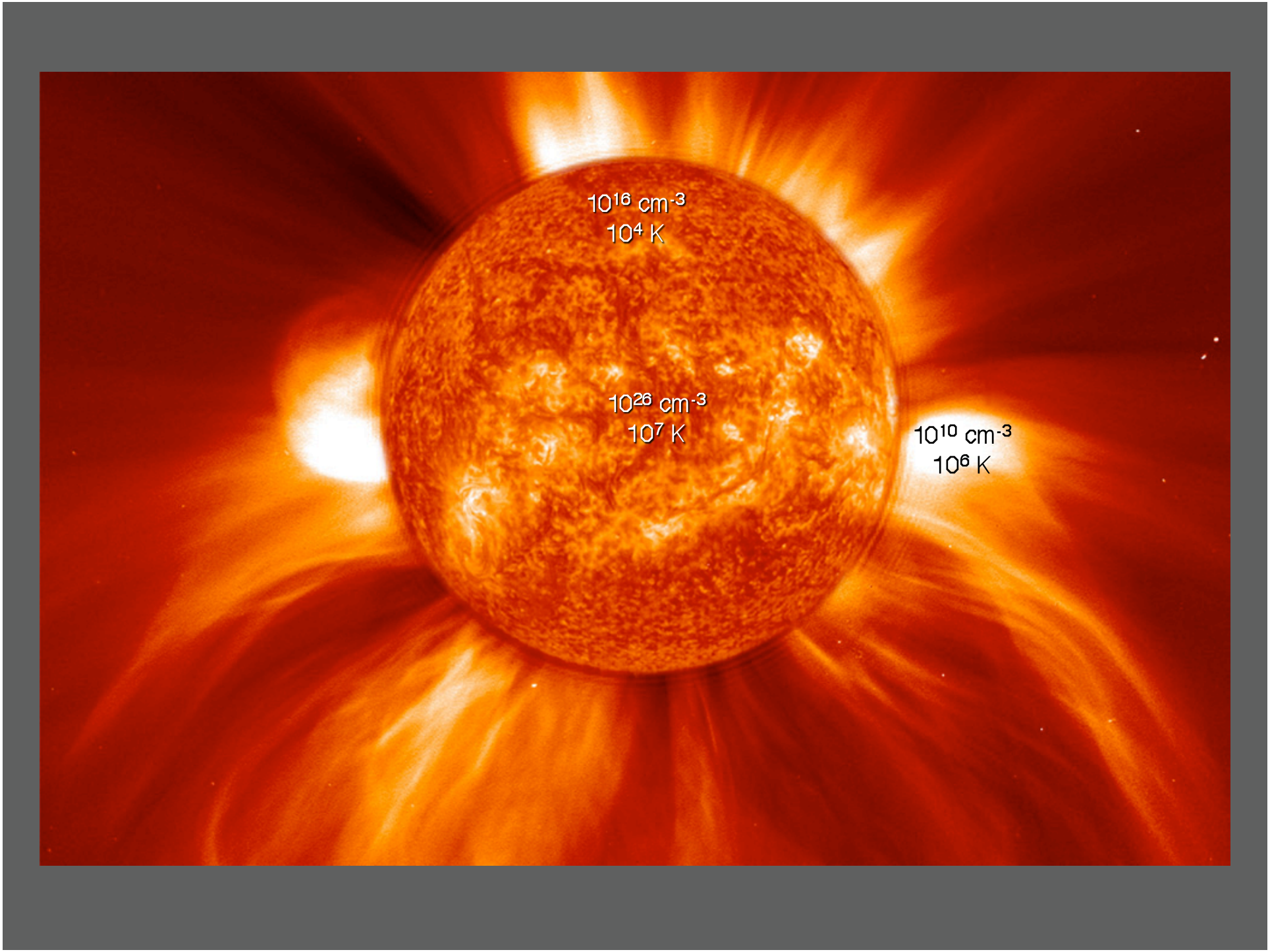
10^{16} cm^{-3}
10^{4} K
10^{26} cm^{-3}
10^{7} K
10^{10} cm^{-3}
10^{6} K

air: $n \sim 3 \times 10^{19}$ cm^{-3}; T ~ 300 K (.025 eV):

$E/V \sim 10^{6}$ ergs cm^{-3}

air: $n \sim 3 \times 10^{19}$ cm^{-3}; T ~ 300 K (.025 eV):

$E/V \sim 10^{6}$ ergs cm^{-3}

center of the Sun: $n \sim 10^{26}$ cm^{-3}; T ~ 10^{7} K (1 keV):

$E/V \sim 10^{17}$ ergs cm^{-3}

surface of the Sun: $n \sim 10^{16}$ cm^{-3}; T ~ 10^{4} K (1 eV):

$E/V \sim 10^{4}$ ergs cm^{-3}

solar corona: $n \sim 10^{10}$ cm^{-3}; T ~ 10^{6} K (0.1 keV):

$E/V \sim 10^{0}$ ergs cm^{-3}

air: $n \sim 3 \times 10^{19}$ cm^{-3}; T ~ 300 K (.025 eV):

$E/V \sim 10^{6}$ ergs cm^{-3}

center of the Sun: $n \sim 10^{26}$ cm^{-3}; T ~ 10^{7} K (1 keV):

$E/V \sim 10^{17}$ ergs cm^{-3}

surface of the Sun: $n \sim 10^{16}$ cm^{-3}; T ~ 10^{4} K (1 eV):

$E/V \sim 10^{4}$ ergs cm^{-3}

solar corona: $n \sim 10^{10}$ cm^{-3}; T ~ 10^{6} K (0.1 keV):

$E/V \sim 10^{0}$ ergs cm^{-3}

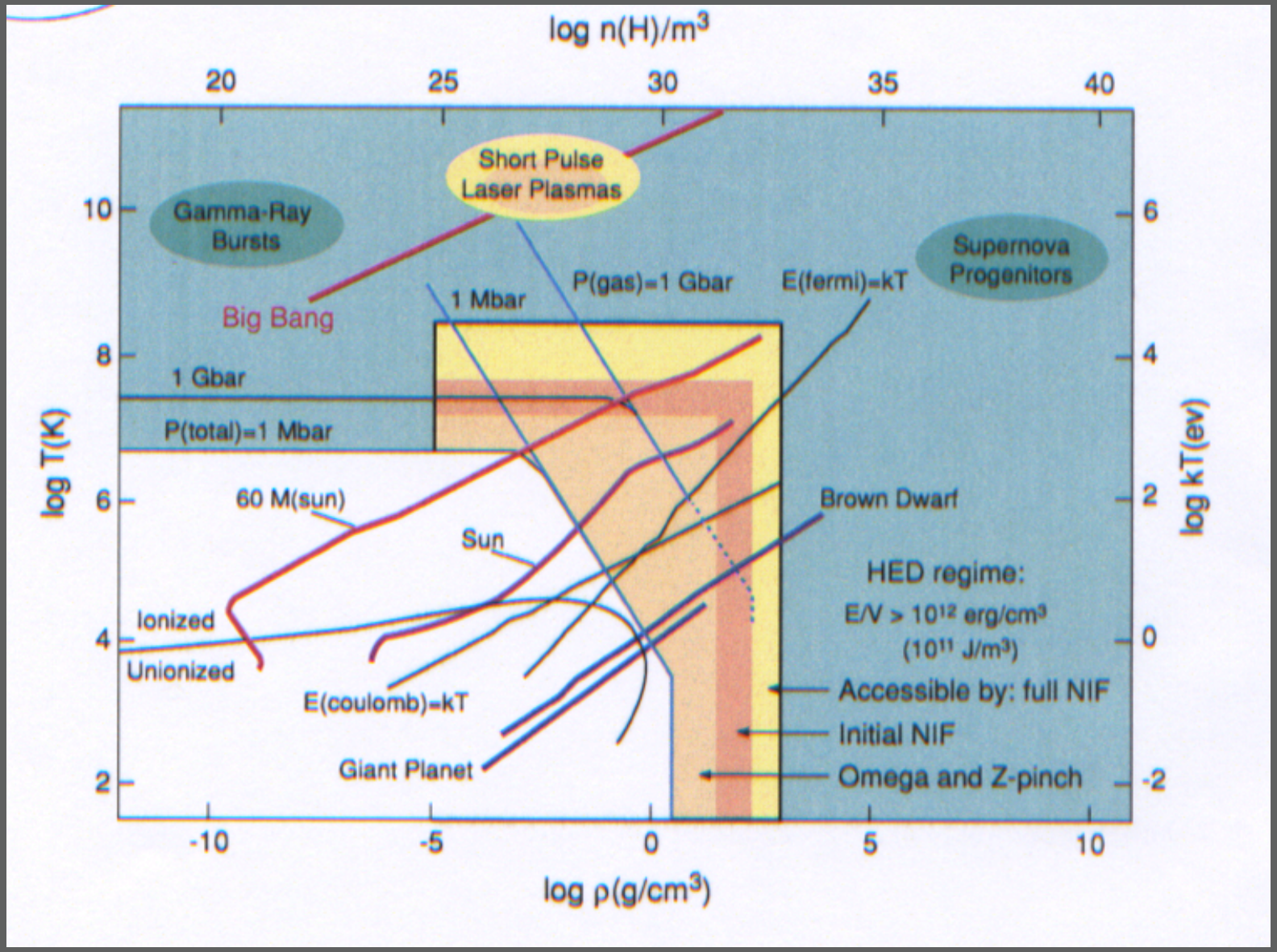
log n(H)/m3
20
25
30
35
40
Short Pulse
Laser Plasmas
Gamma-Ray
Bursts
Supernova
Progenitors
P(gas)=1 Gbar
E(fermi)=kT
1 Mbar
Big Bang
1 Gbar
P(total)=1 Mbar
60 M(sun)
Sun
Brown Dwarf
HED regime:
E/V > 10^12 erg/cm^3
(10^11 J/m^3)
Ionized
Unionized
E(coulomb)=kT
Accessible by: full NIF
Initial NIF
Omega and Z-pinch
Giant Planet
log T(K)
log kT(ev)
10
8
6
4
2
6
4
2
0
-2
-10
-5
0
5
10
log ρ(g/cm3)

Controlled **fusion** is a major motivator

High density and temperature are required

60 beams: 30 kJ: 1 ns: 30 TW

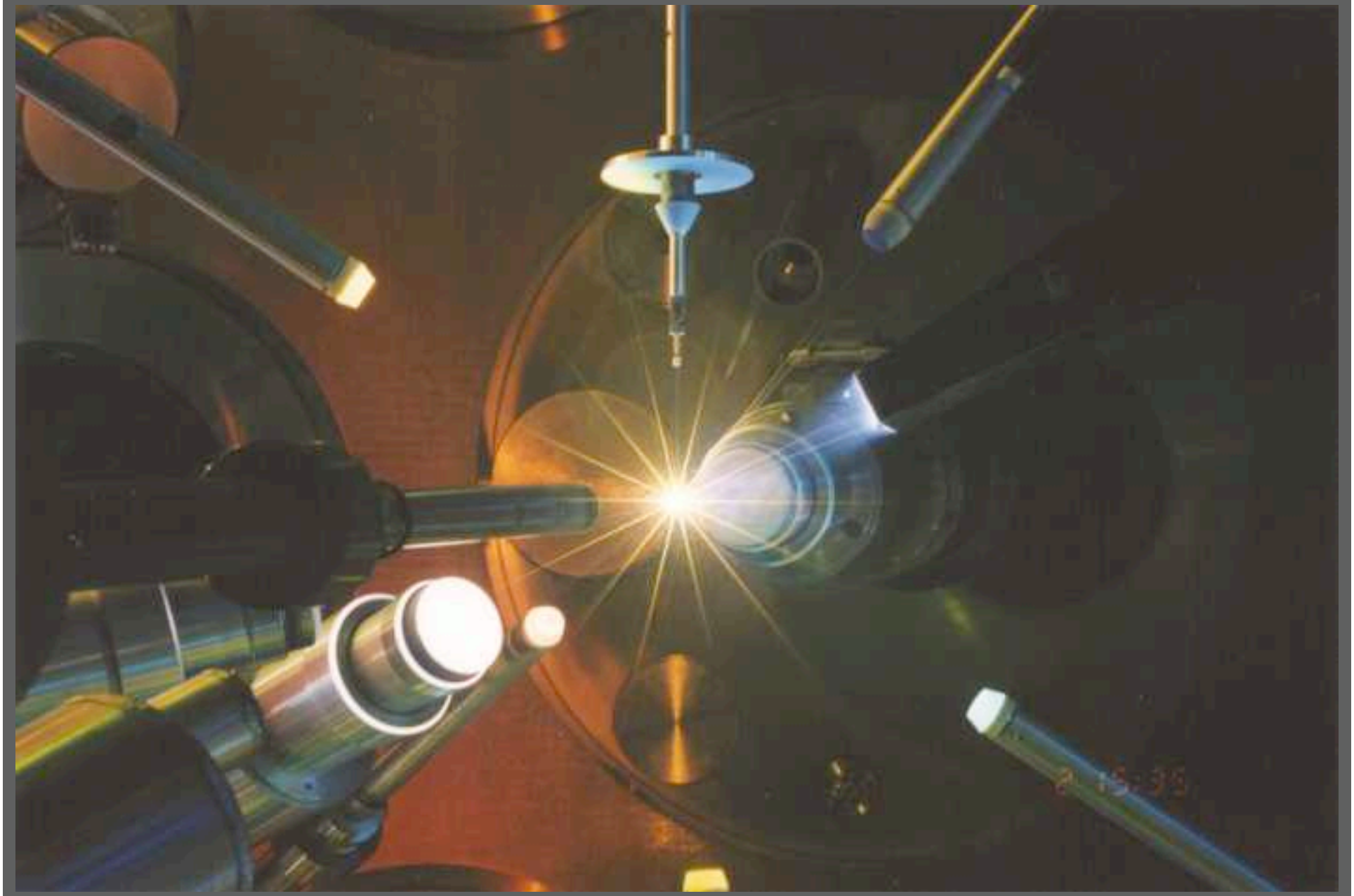

Inertial confinement fusion – compressing and heating a hydrogen-filled capsule

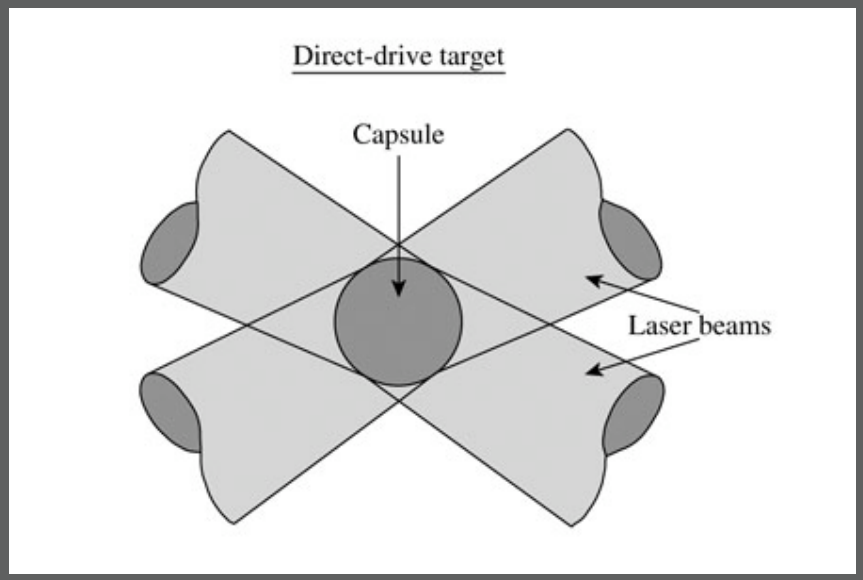

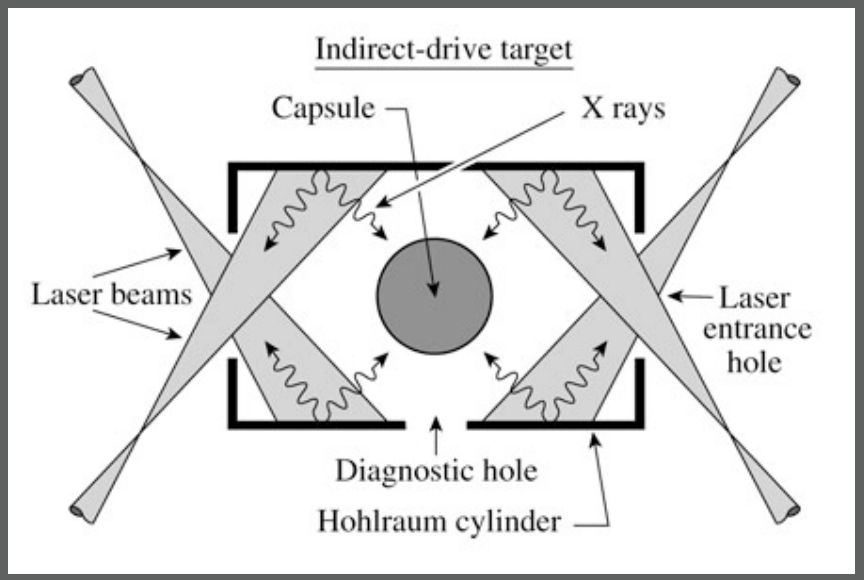

Gold **hohlraum** – converts laser light to thermal x-rays

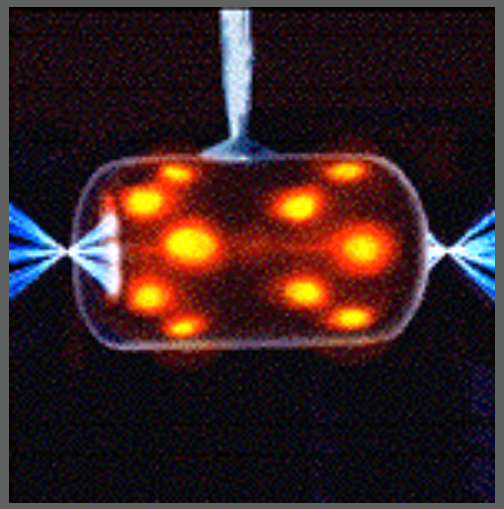

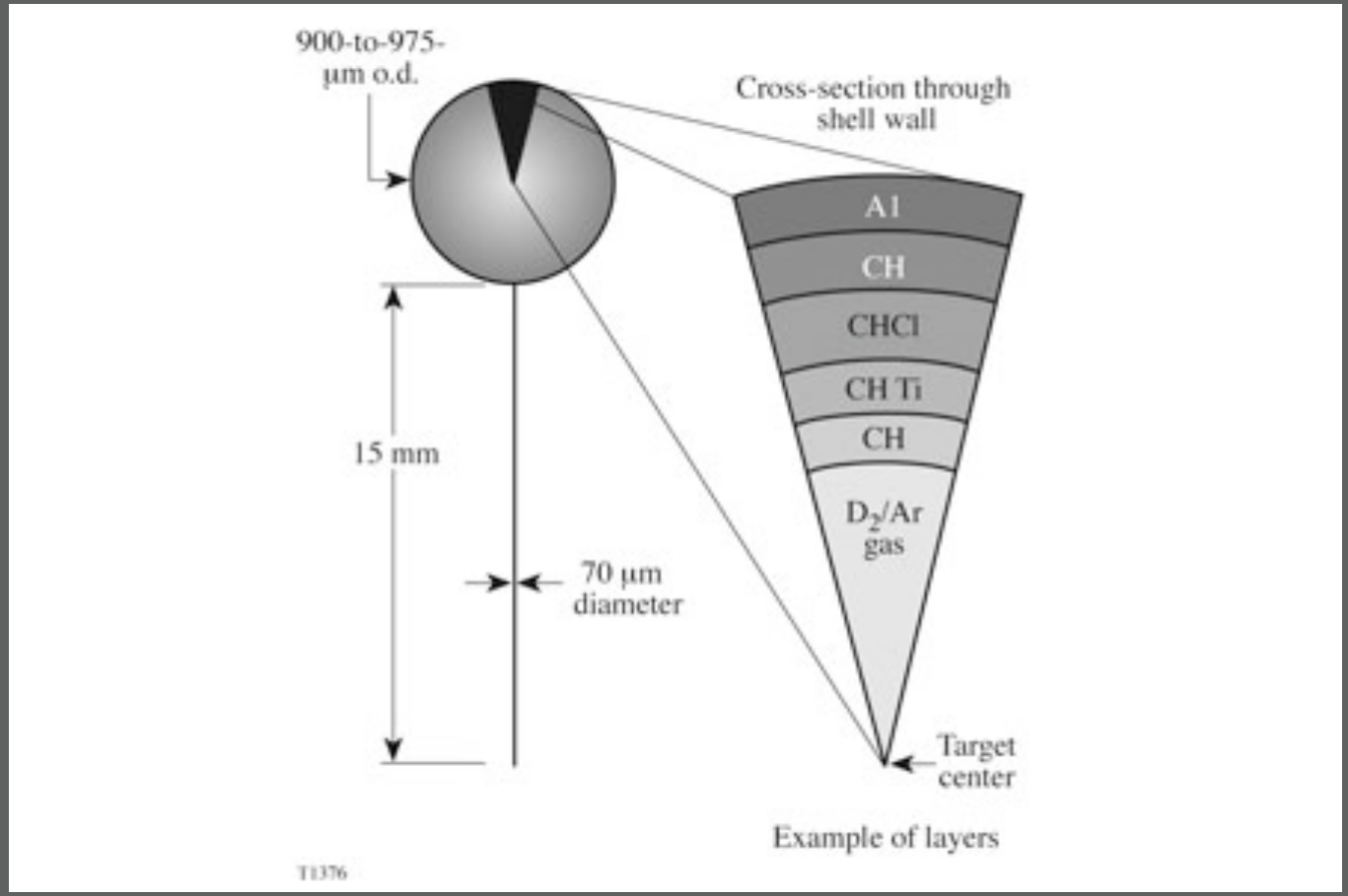
900-to-975-
μm o.d.
Cross-section through
shell wall
Al
CH
CHCl
CH Ti
CH
D_2/Ar
gas
15 mm
70 μm
diameter
Target
center
Example of layers
T1376

Outer layer is ablated, conservation of momentum…

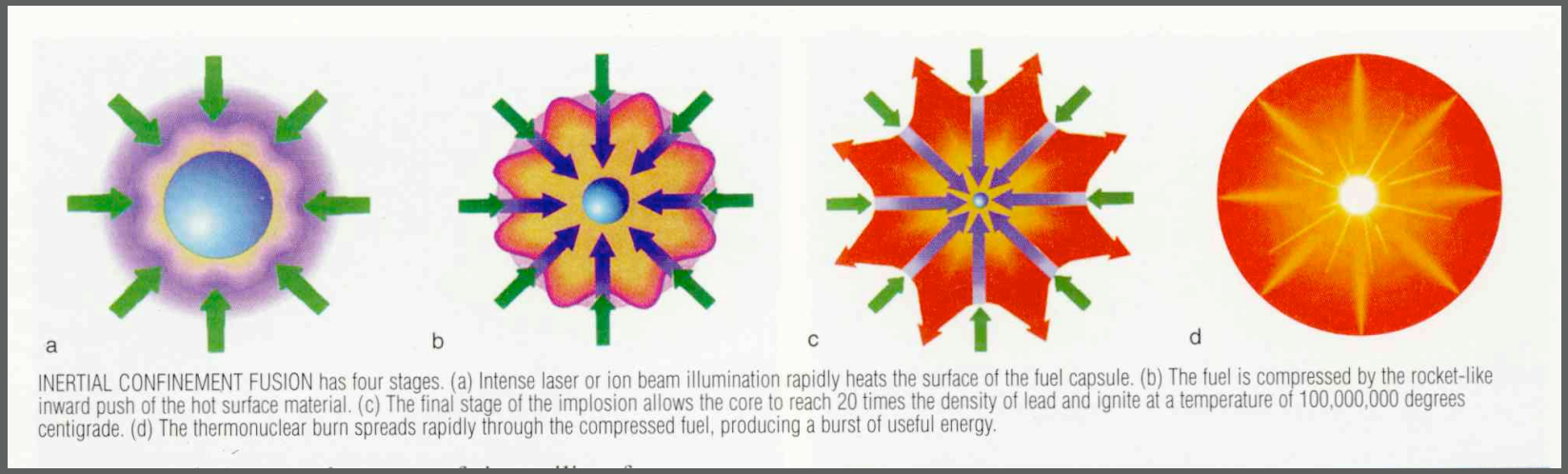

INERTIAL CONFINEMENT FUSION has four stages. (a) Intense laser or ion beam illumination rapidly heats the surface of the fuel capsule. (b) The fuel is compressed by the rocket-like inward push of the hot surface material. (c) The final stage of the implosion allows the core to reach 20 times the density of lead and ignite at a temperature of 100,000,000 degrees centigrade. (d) The thermonuclear burn spreads rapidly through the compressed fuel, producing a burst of useful energy.

…compresses the core of the capsule

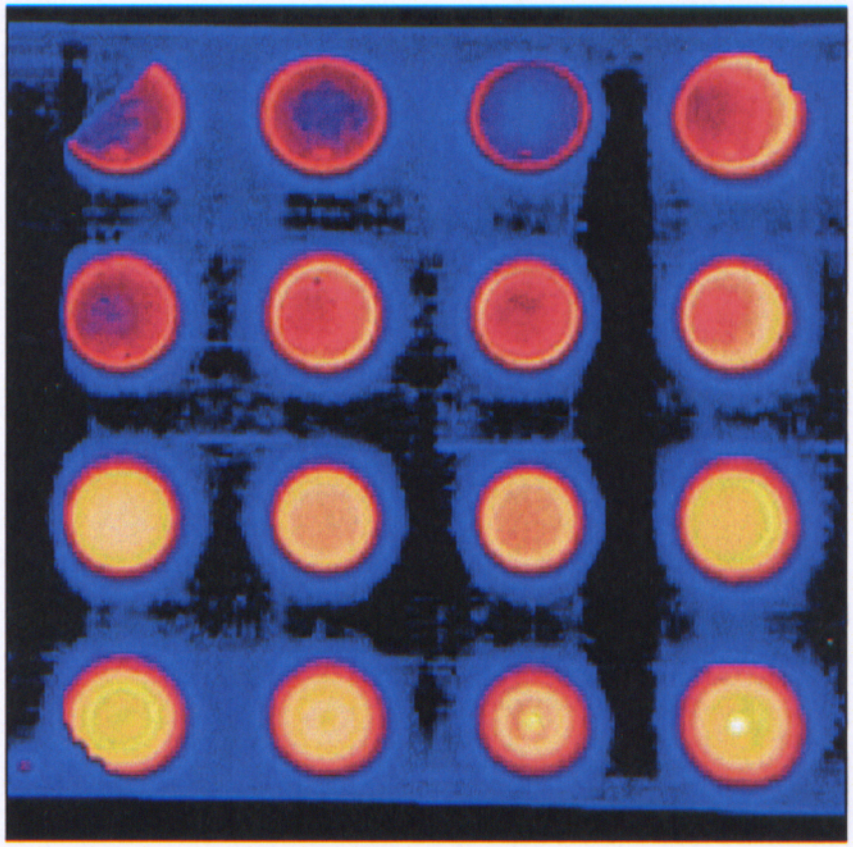

FIGURE 3.1 X-ray pinhole camera "movie" of a directly driven inertial confinement fusion implosion on the OMEGA laser system, from the laser irradiating the shell at early times, to the formation of a hot spot. Each image has ~50-ps temporal resolution, and the total duration of the "movie" is ~3.2 ns. The initial target diameter (upper left image) is ~1 mm, and the final compressed core diameter (third image, bottom row) is <100 μm. Courtesy of the Laboratory for Laser Energetics, University of Rochester.

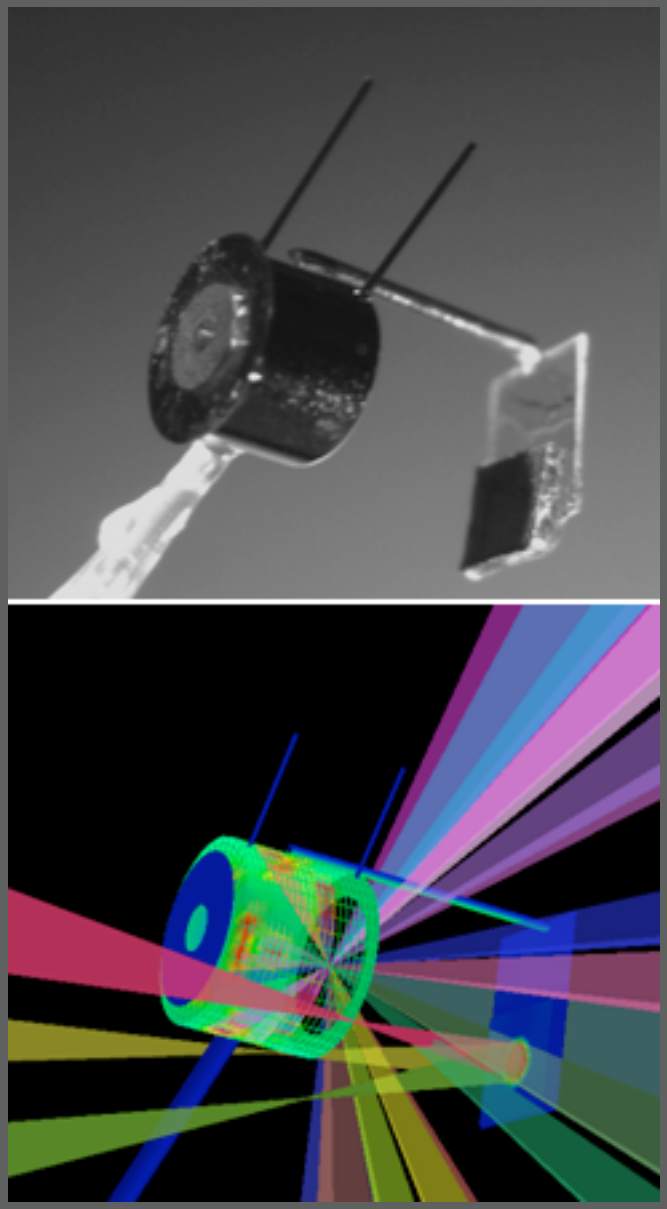

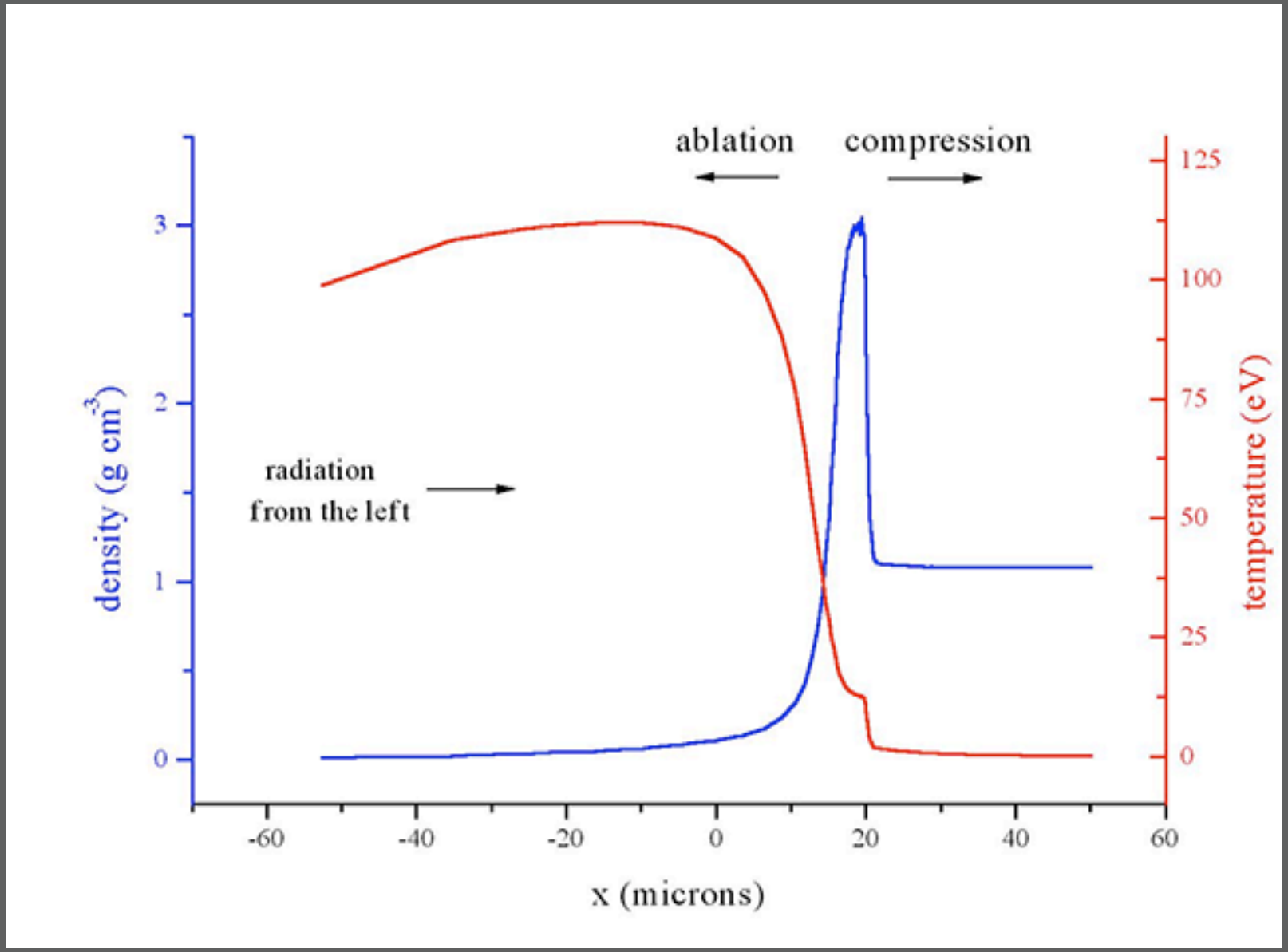
ablation
compression
radiation
from the left
density (g cm-3)
temperature (eV)
x (microns)
0
1
2
3
-60
-40
-20
0
20
40
60
0
25
50
75
100
125

Therefore, the three equations of fluid mechanics are:

$$\frac{\partial \rho}{\partial t} + \frac{\partial}{\partial x}(\rho u_x) = 0 \qquad \frac{\partial \rho}{\partial t} + \nabla . (\rho \mathbf{u}) = 0$$

$$\rho \left(\frac{\partial u_x}{\partial t} + u_x \frac{\partial u_x}{\partial x} \right) = -\frac{\partial P}{\partial x} \qquad \rho \left[\frac{\partial \mathbf{u}}{\partial t} + (\mathbf{u} . \nabla)\mathbf{u} \right] = -\nabla P$$

$$T \left(\frac{\partial s}{\partial t} + u_x \frac{\partial s}{\partial x} \right) = \epsilon \qquad T \left[\frac{\partial s}{\partial t} + (\mathbf{u} . \nabla) s \right] = \epsilon$$

(one-dimensional) (three-dimensional)

Pressure disturbance -> sound wave

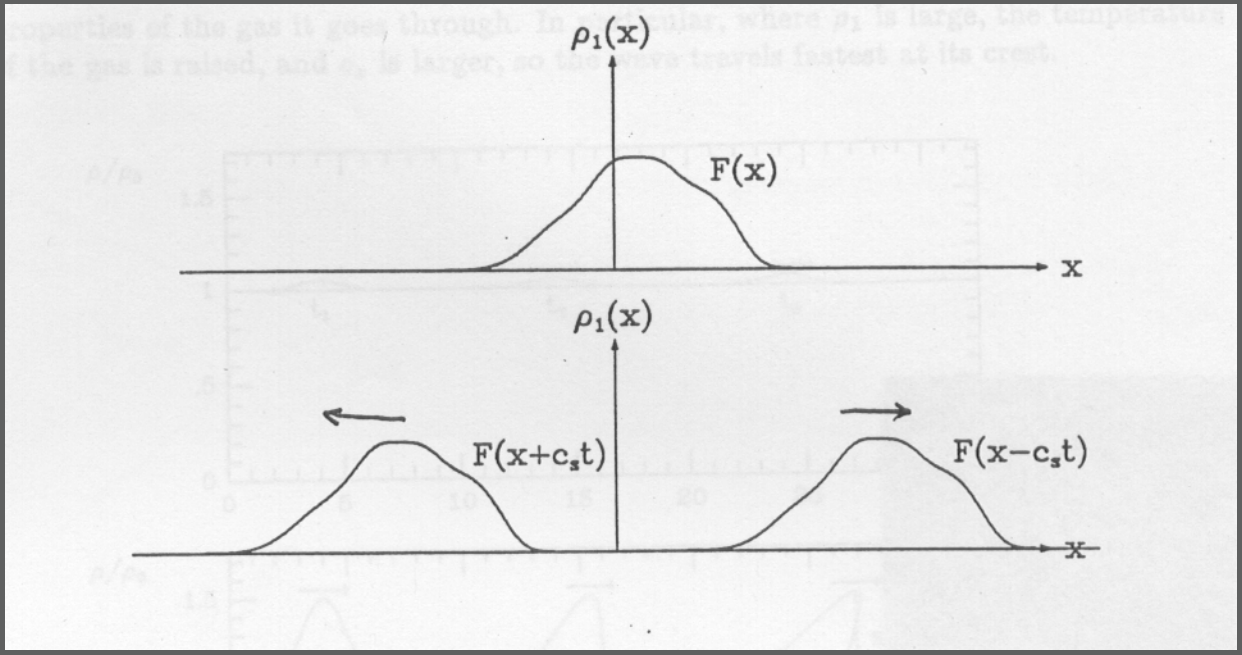

Supersonic disturbance: shock wave

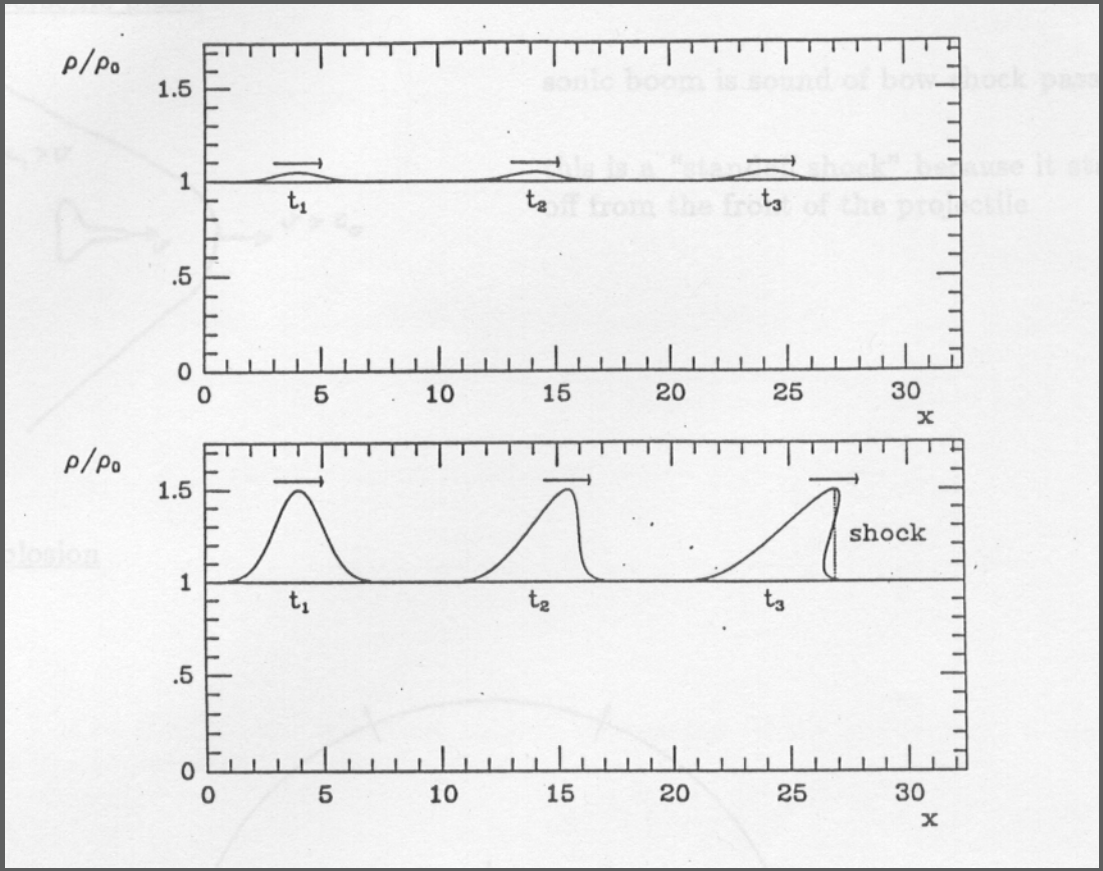

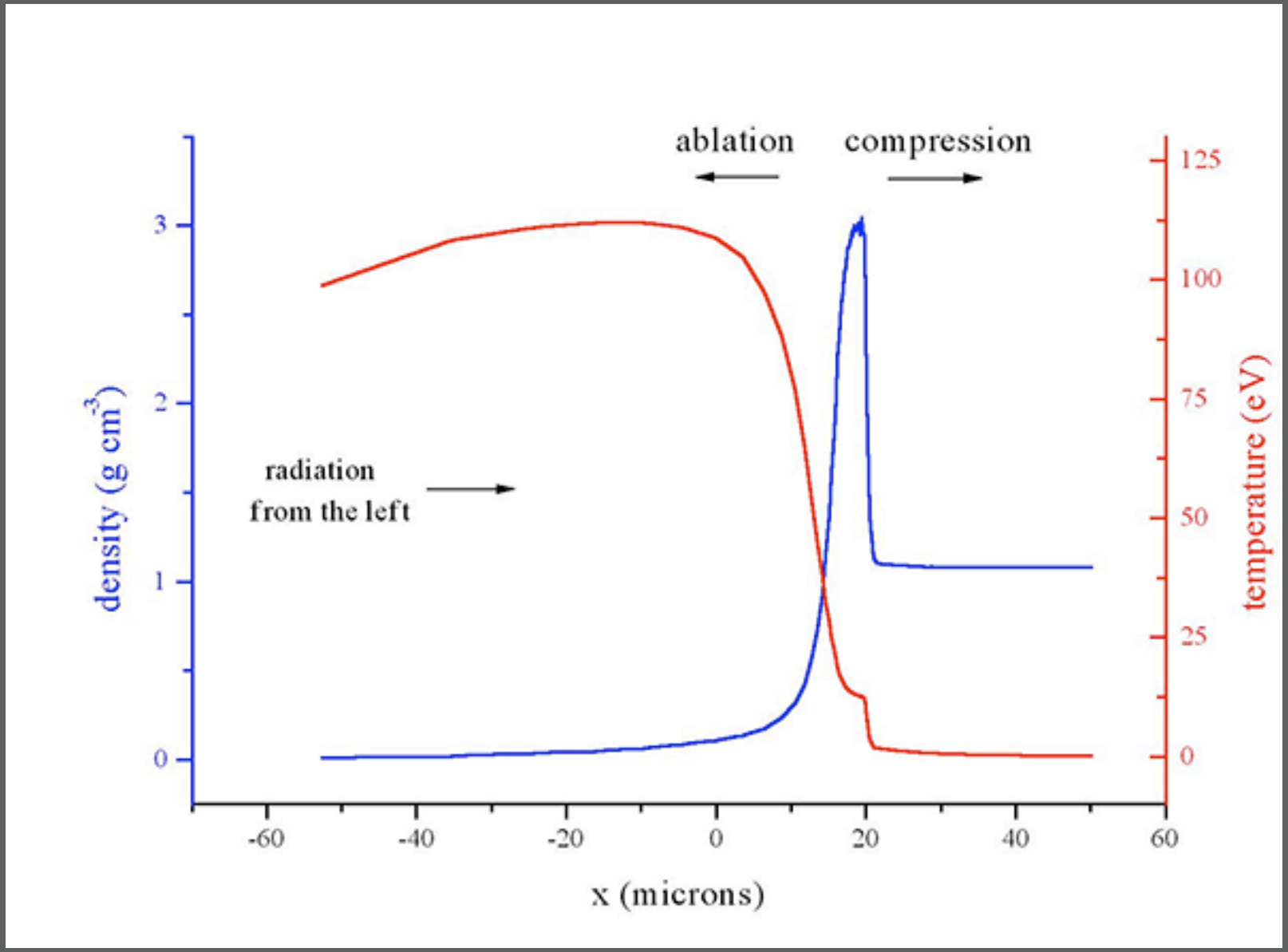
ablation
compression
radiation
from the left
density (g cm-3)
temperature (eV)
x (microns)
0
1
2
3
-60
-40
-20
0
20
40
60
0
25
50
75
100
125

NIF: National Ignition Facility
@ Livermore National Laboratory in California

192 beams: 1.8 MJ: <1ns: PW (petawatt = 10^{15} W)

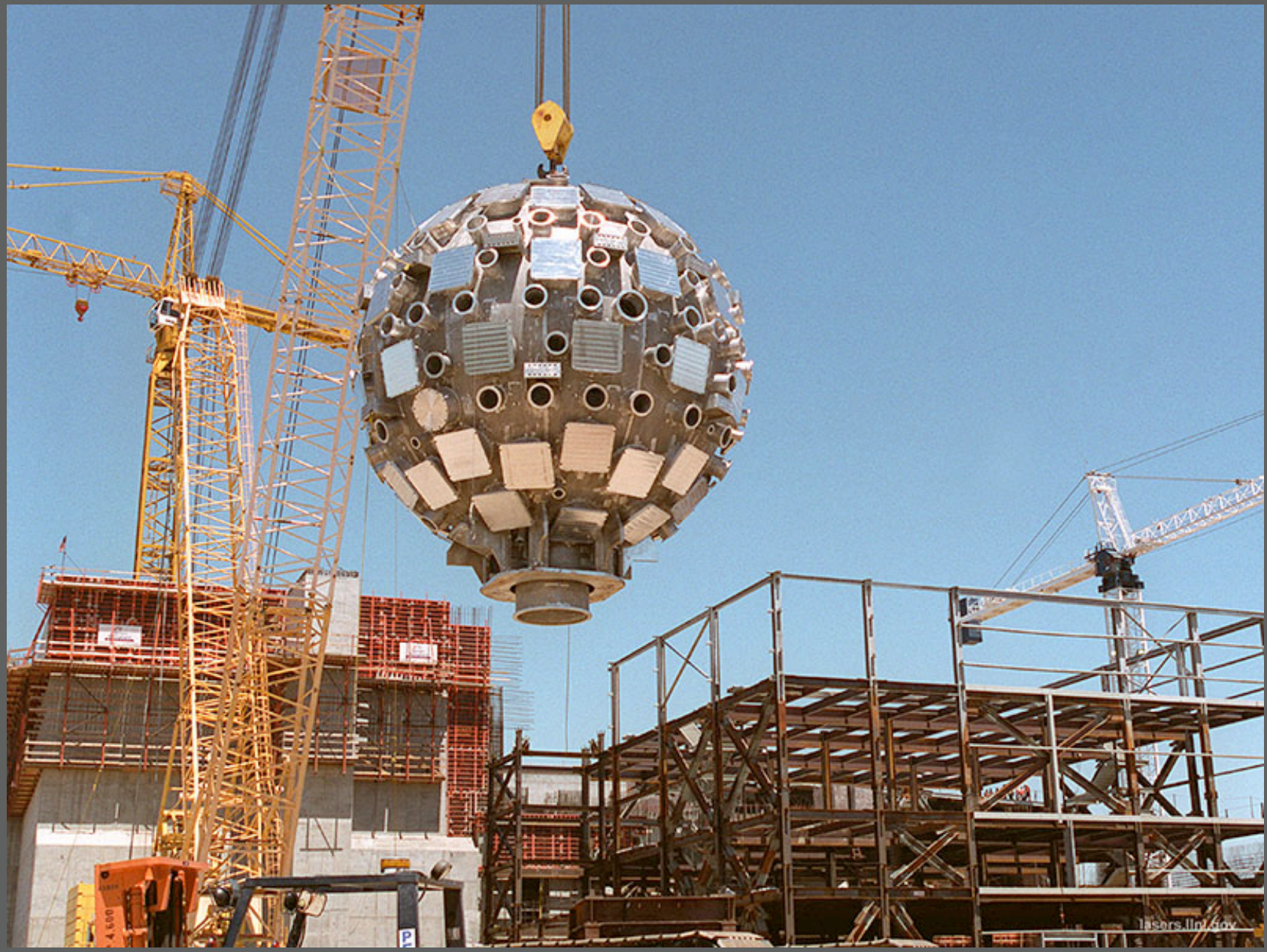

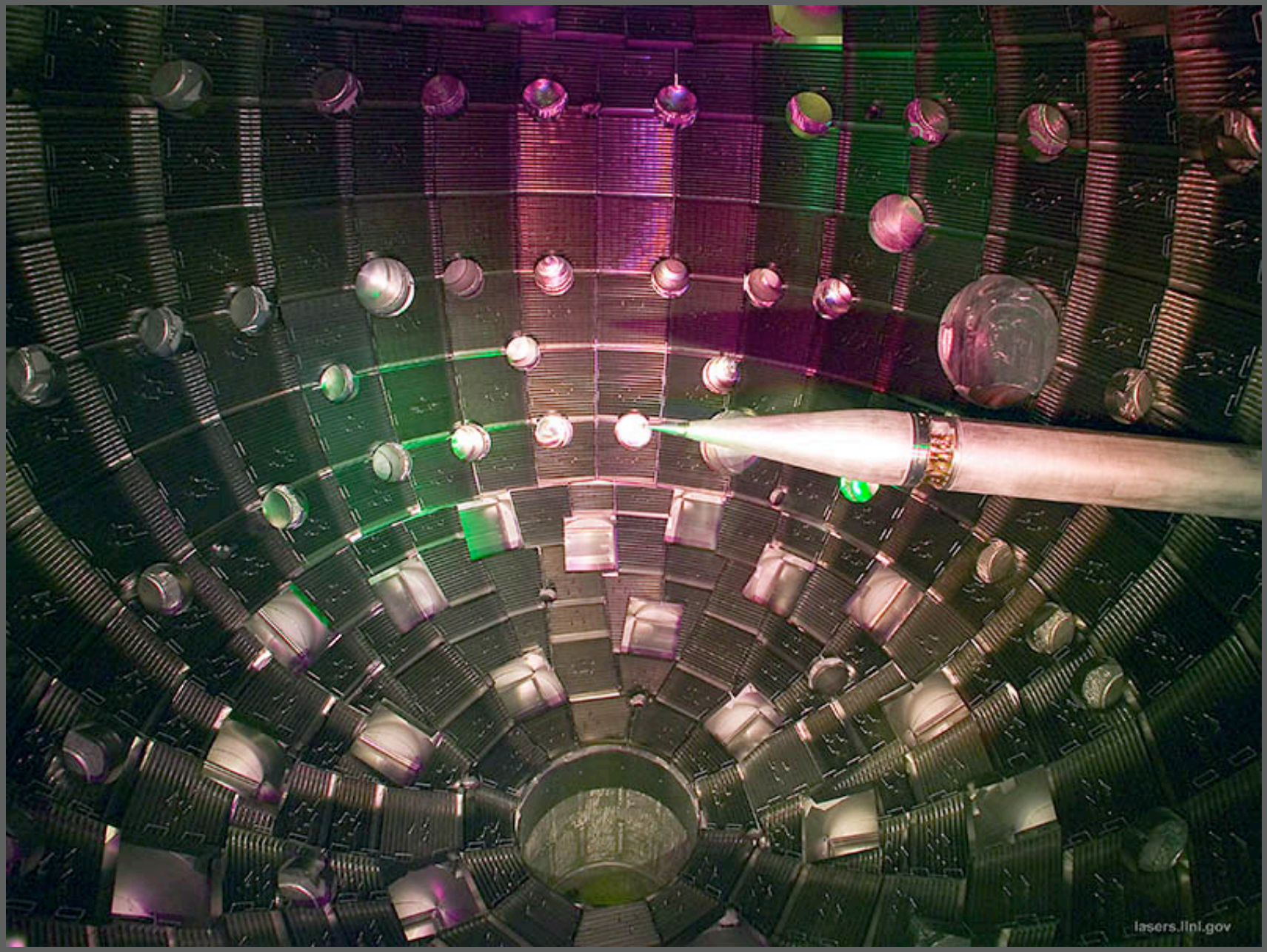
lasers.llnl.gov

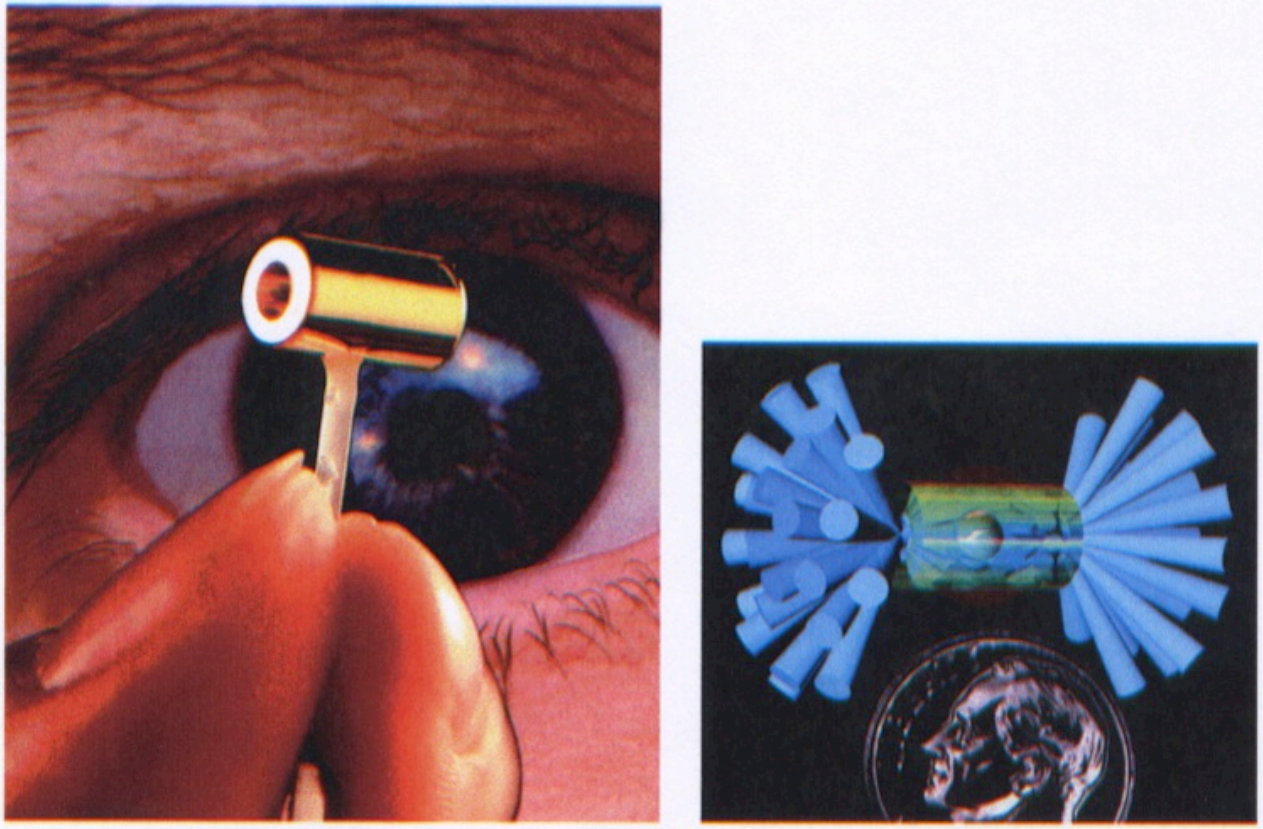

FIGURE 4.3 Images of the type of hohlraum used for ignition experiments. The schematic on the right shows the hohlraum irradiated by 192 NIF beams. Courtesy of Lawrence Livermore National Laboratory.

Astrophysics applications

Astrophysical data

Experimental data

Numerical simulations

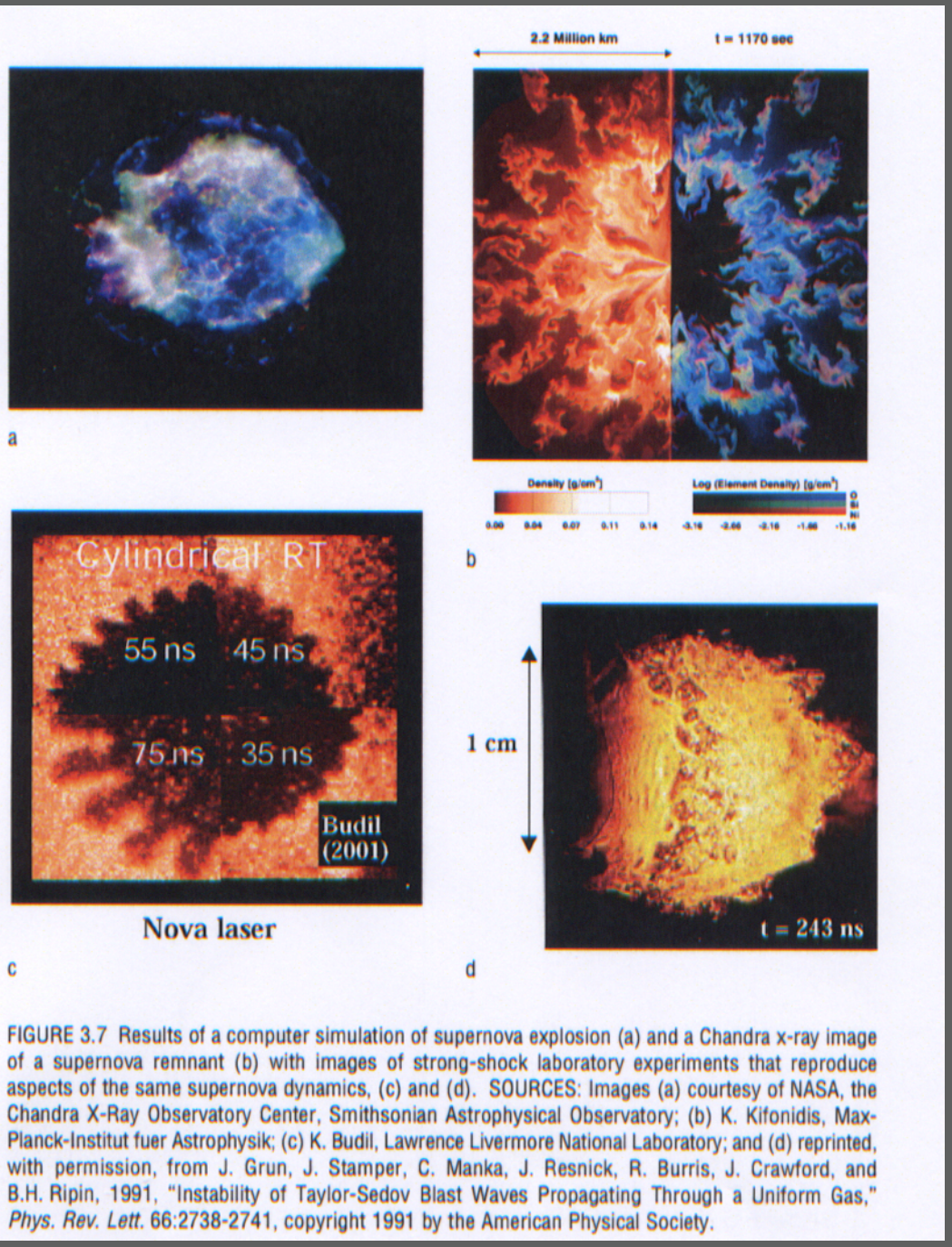

FIGURE 3.7 Results of a computer simulation of supernova explosion (a) and a Chandra x-ray image of a supernova remnant (b) with images of strong-shock laboratory experiments that reproduce aspects of the same supernova dynamics, (c) and (d). SOURCES: Images (a) courtesy of NASA, the Chandra X-Ray Observatory Center, Smithsonian Astrophysical Observatory; (b) K. Kifonidis, Max-Planck-Institut fuer Astrophysik; (c) K. Budil, Lawrence Livermore National Laboratory; and (d) reprinted, with permission, from J. Grun, J. Stamper, C. Manka, J. Resnick, R. Burris, J. Crawford, and B.H. Ripin, 1991, "Instability of Taylor-Sedov Blast Waves Propagating Through a Uniform Gas," *Phys. Rev. Lett.* 66:2738-2741, copyright 1991 by the American Physical Society.

Supernova remnant: Hubble data (left); laboratory experiment (right)

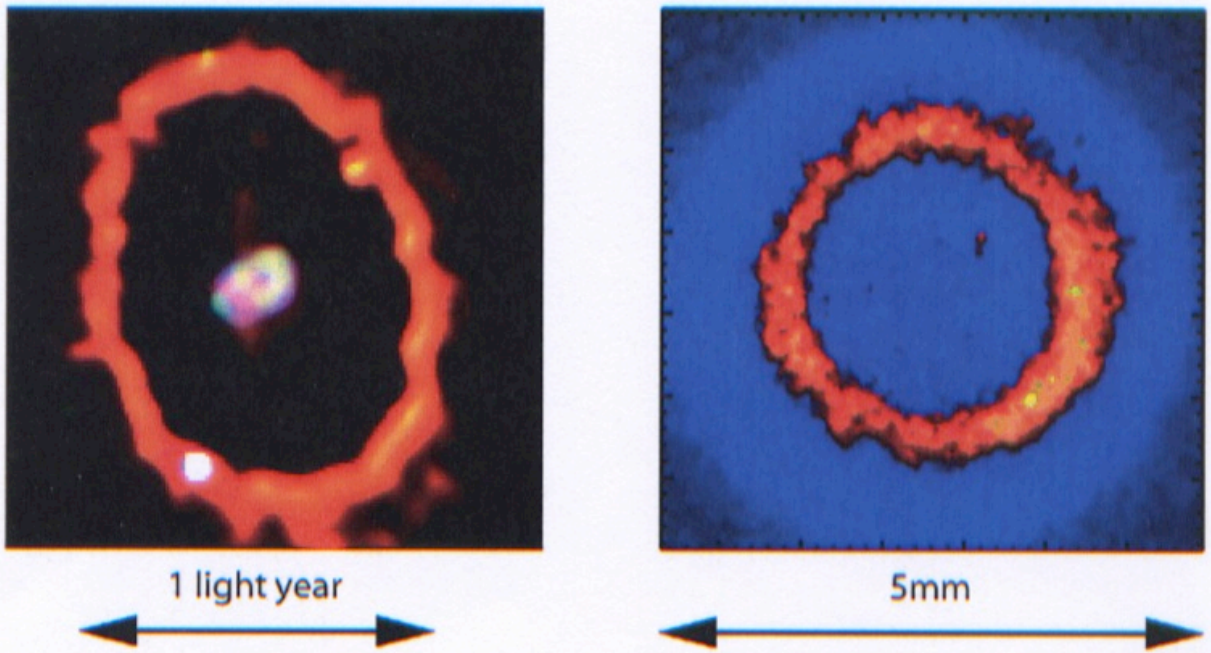

FIGURE 3.8 An example of a strongly radiative, cylindrical shock from Z is shown (right), juxtaposed with the glowing shocked circumstellar nebula of Supernova 1987A remnant (left). Courtesy of (left) P. Garnavich, Harvard-Smithsonian Center for Astrophysics and NASA; and (right) J. Bailey, Sandia National Laboratories.

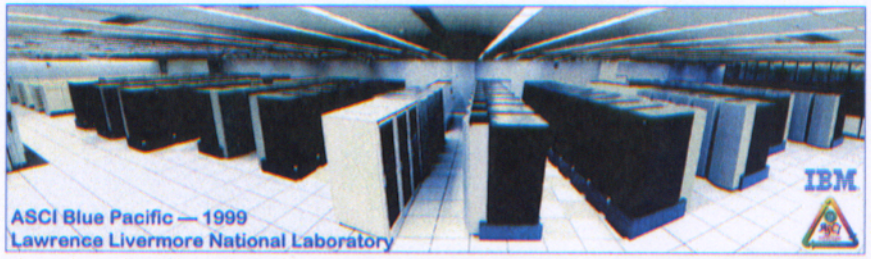

a

b

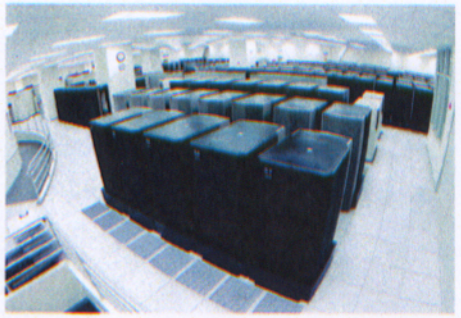

c

d

e

FIGURE 4.12 Five top supercomputer sites as of November 2001. (a) ASCI Blue-Pacific at Lawrence Livermore National Laboratory is an IBM SP 604e machine capable of 2.14 Tflops; (b) the Terascale System at the Pittsburgh Supercomputing Center is a Compaq Alpha Server machine capable of 4.05 Tflops; (c) the National Energy Research Scientific Computing (NERSC) center at the Lawrence Berkeley National Laboratory is an IBM SP Power3 machine capable of 3.05 Tflops; (d) ASCI Red at Sandia National Laboratories is an Intel processor-based machine capable of 2.37 Tflops; and (e) ASCI White at Lawrence Livermore National Laboratory is an IBM SP Power3 machine capable of 7.22 Tflops. Courtesy of (a) Lawrence Livermore National Laboratory, (b) The Pittsburgh Computer Center; (c) Lawrence Berkeley National Laboratory, (d) Sandia National Laboratories, and (e) Lawrence Livermore National Laboratory.

Equation of state (EOS):
Relationship among pressure, density, temperature

If we try to compress material, how do these three properties change in concert?

Different models of hydrogen EOS: applications to the interior of Jupiter

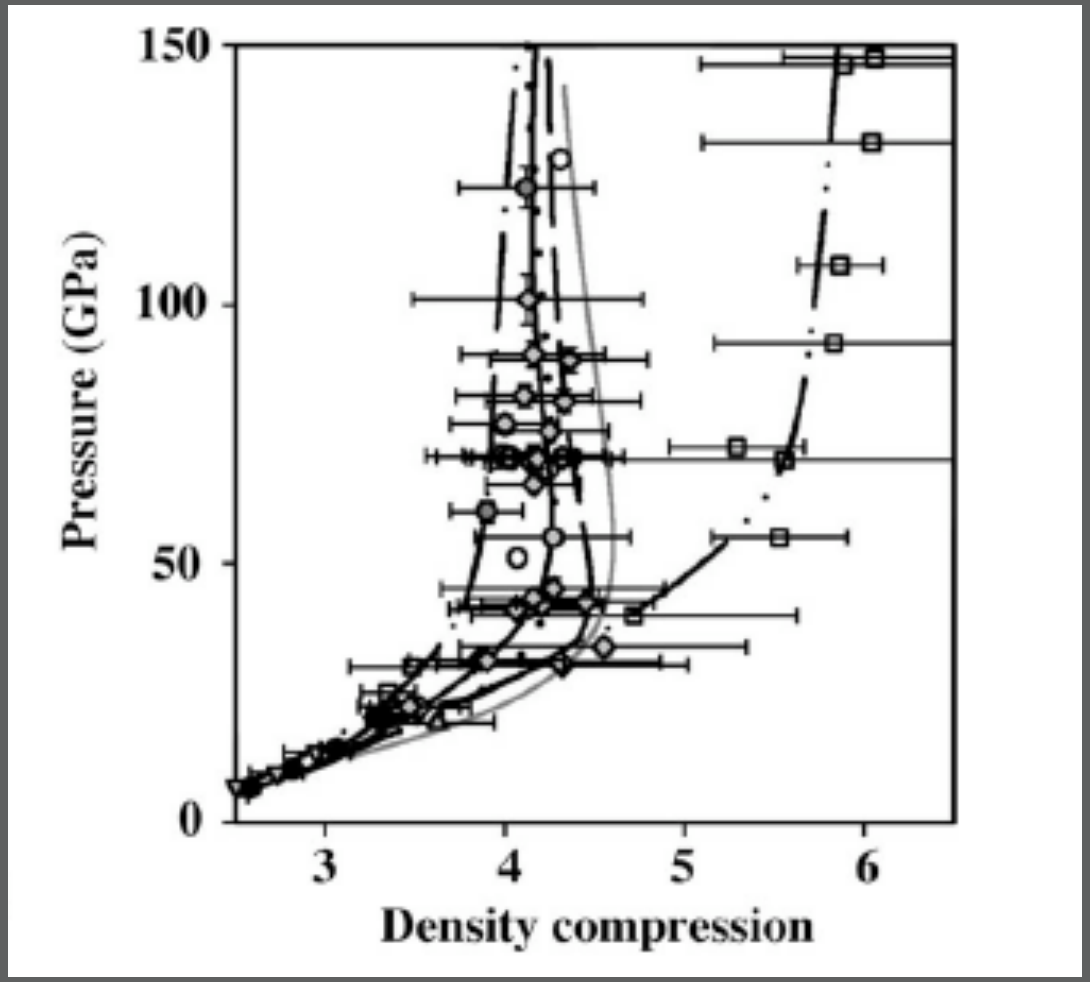

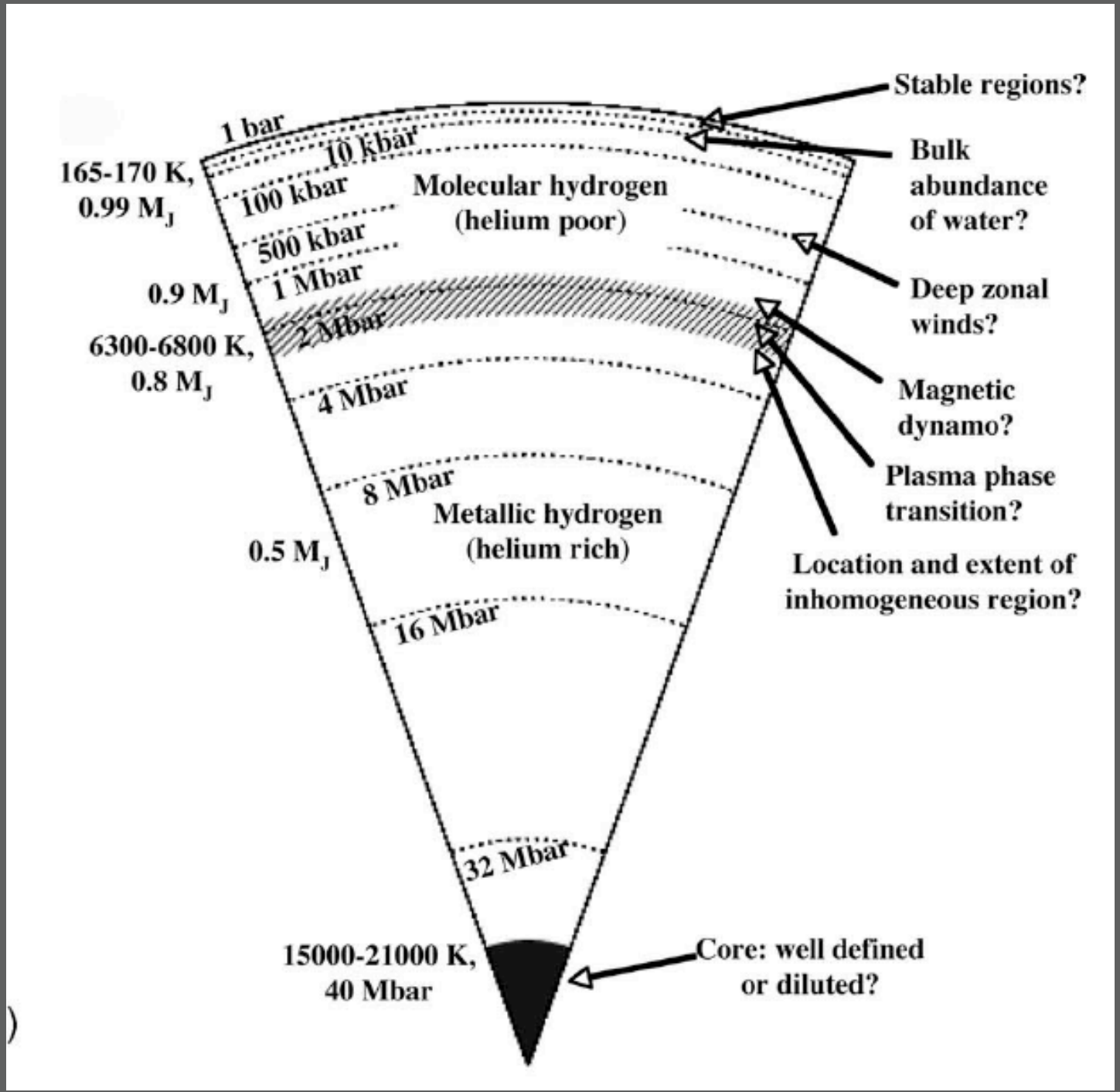
Stable regions?
1 bar
10 kbar
165-170 K,
0.99 M_J
100 kbar
Molecular hydrogen
(helium poor)
Bulk
abundance
of water?
500 kbar
1 Mbar
0.9 M_J
Deep zonal
winds?
2 Mbar
6300-6800 K,
0.8 M_J
4 Mbar
Magnetic
dynamo?
8 Mbar
Plasma phase
transition?
Metallic hydrogen
(helium rich)
0.5 M_J
Location and extent of
inhomogeneous region?
16 Mbar
32 Mbar
15000-21000 K,
40 Mbar
Core: well defined
or diluted?

Empirical Models of Pressure and Density in Saturn's Interior: Implications for the Helium Concentration, its Depth Dependence, and Saturn's Precession Rate

Ravit Helled[1,**], Gerald Schubert[1], and John D. Anderson[2]

[1]Department of Earth and Space Sciences and Institute of Geophysics and Planetary Physics,

University of California, Los Angeles, CA 900951567, USA

[2]Jet Propulsion Laboratory

California Institute of Technology, Pasadena, CA 91109

[**] *corresponding author, E-mail address: rhelled@ess.ucla.edu*

Abstract

We present 'empirical' models (pressure vs. density) of Saturn's interior constrained by the gravitational coefficients J_2, J_4, and J_6 for different assumed rotation rates of the planet. The empirical pressure-density profile is interpreted in terms of a hydrogen and helium physical equation of state to deduce the hydrogen to helium ratio in Saturn and to constrain the depth dependence of helium and heavy element abundances. The planet's internal structure (pressure vs. density) and composition are found to be insensitive to the assumed rotation rate for periods between 10h:32m:35s and 10h:41m:35s. We find that helium is depleted in the upper envelope, while in the high pressure region ($P \gtrsim 1$ Mbar) either the helium abundance or the concentration of heavier elements is significantly enhanced. Taking the ratio of hydrogen to helium in Saturn to be solar, we find that the maximum mass of heavy elements in Saturn's interior ranges from ~ 6 to 20 $M_\oplus$.

The empirical models of Saturn's interior yield a moment of inertia factor varying from 0.22271 to 0.22599 for rotation periods between 10h:32m:35s and 10h:41m:35s, respectively. A long-term precession rate of about 0.754" yr^{-1} is found to be consistent with the derived moment of inertia values and assumed rotation rates over the entire range of investigated rotation rates. This suggests that the long-term precession period of Saturn is somewhat shorter than the generally assumed value of 1.77×10^6 years inferred from modeling and observations.

Key Words SATURN; SATURN, INTERIOR; ABUNDANCES, INTERIORS

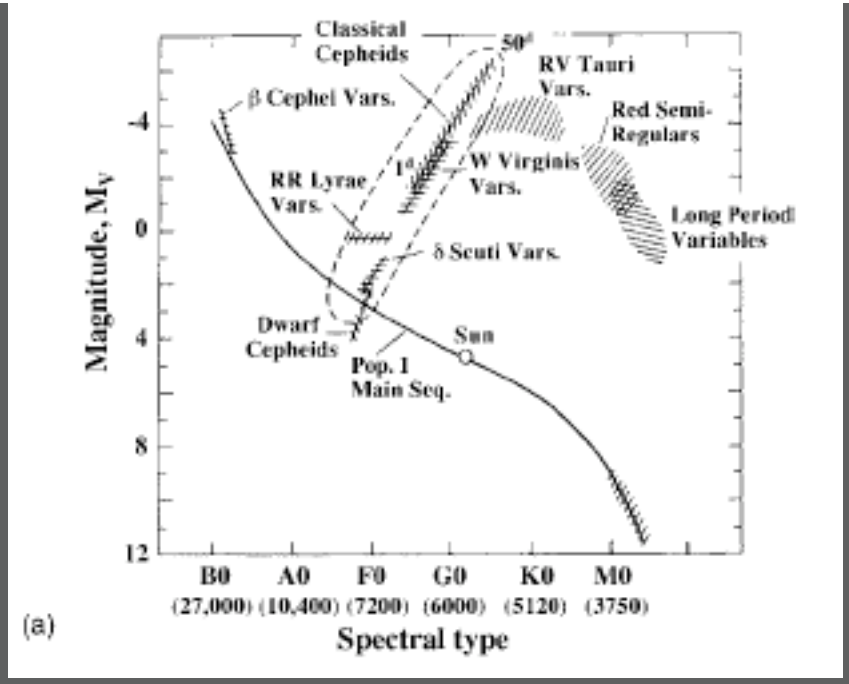

Stars pulsate:
Opacity (cm^2/g) plays a key role in trapping energy

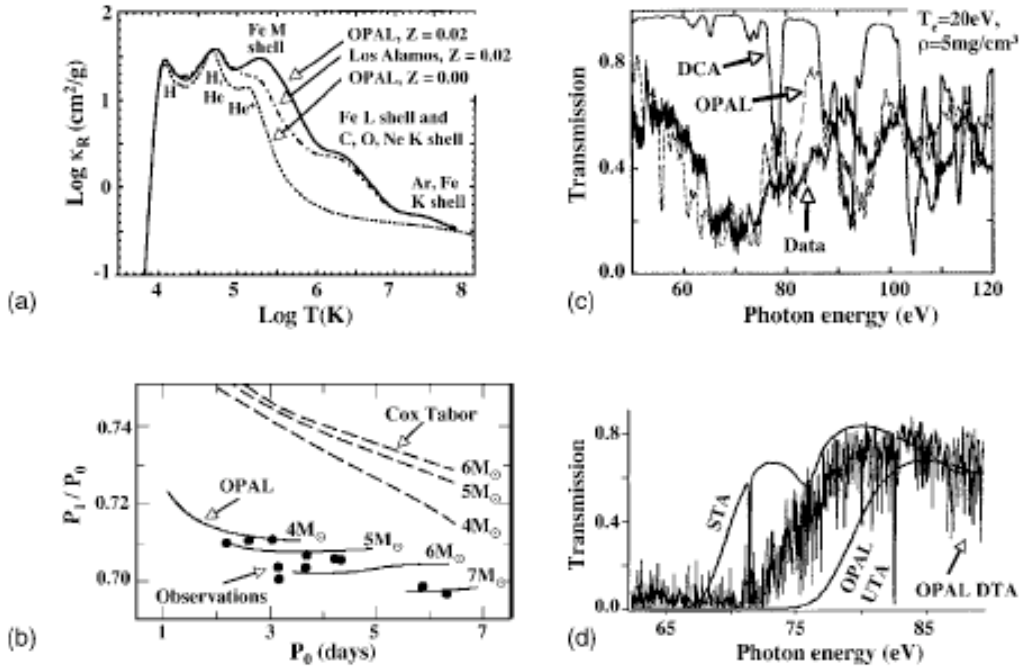

Astrophysical jets

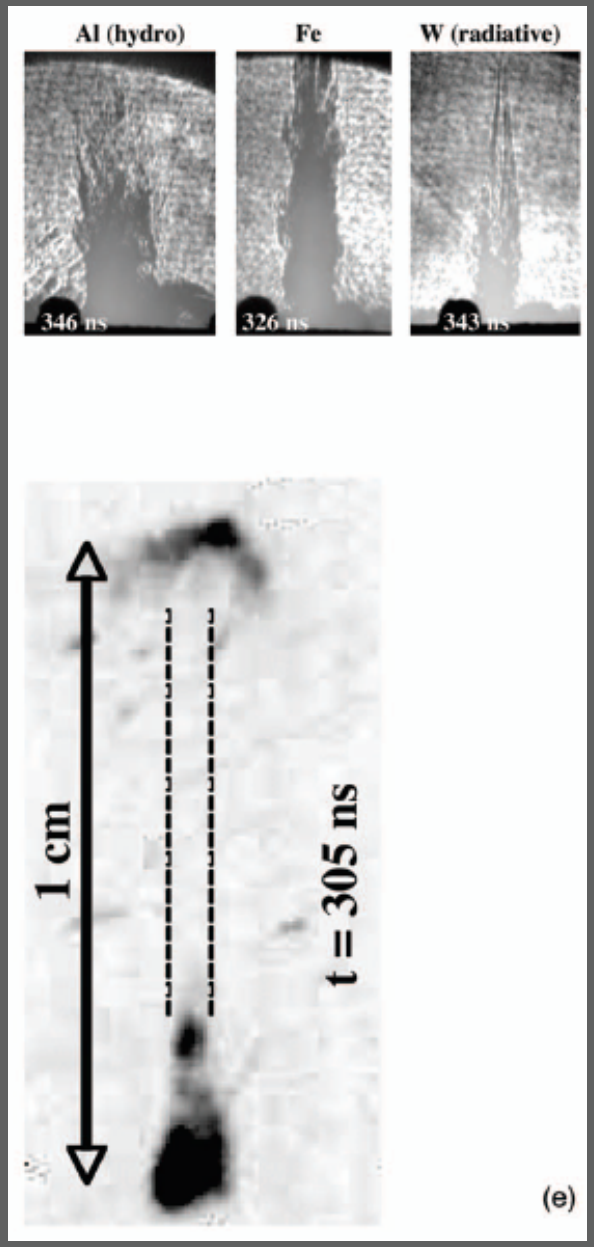

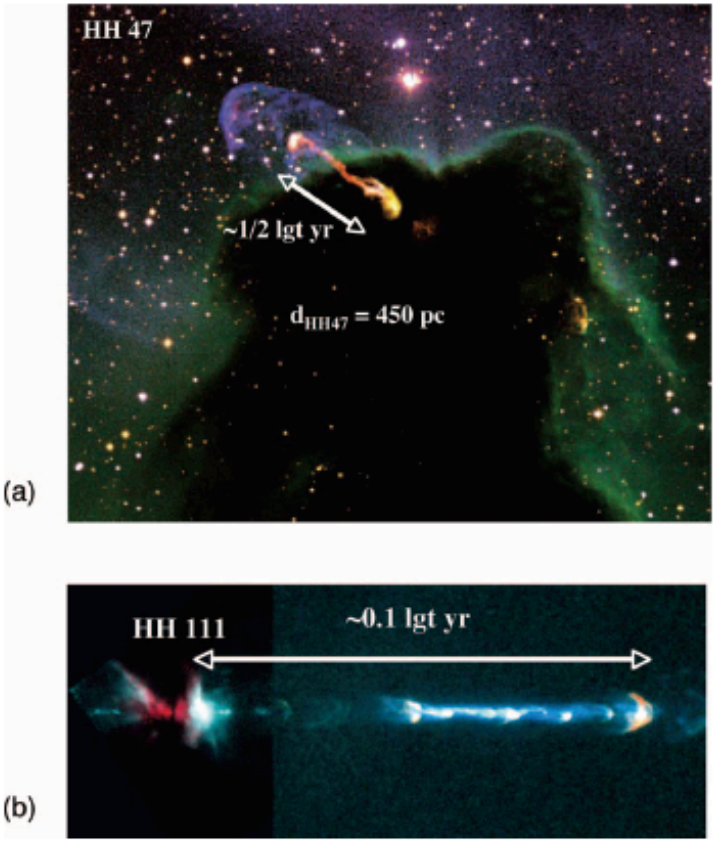

FIG. 24. (Color) Jets from young stellar objects in the galaxy. (a) Optical image of the protostellar jet, Herbig-Haro (HH) 47. The bipolar HH 47 complex embedded in the dense Bok Globule 1500 light years away at the edge of the Gum Nebula: (red) [SII] emission; (green) Hα, (blue) [OIII]. (b) Optical image of the jet, HH 111. Adapted from Reipurth and Bally, 2001.

Hydrodynamic instabilities

Rayleigh-Taylor instability

low-density fluid pushes a high-density fluid

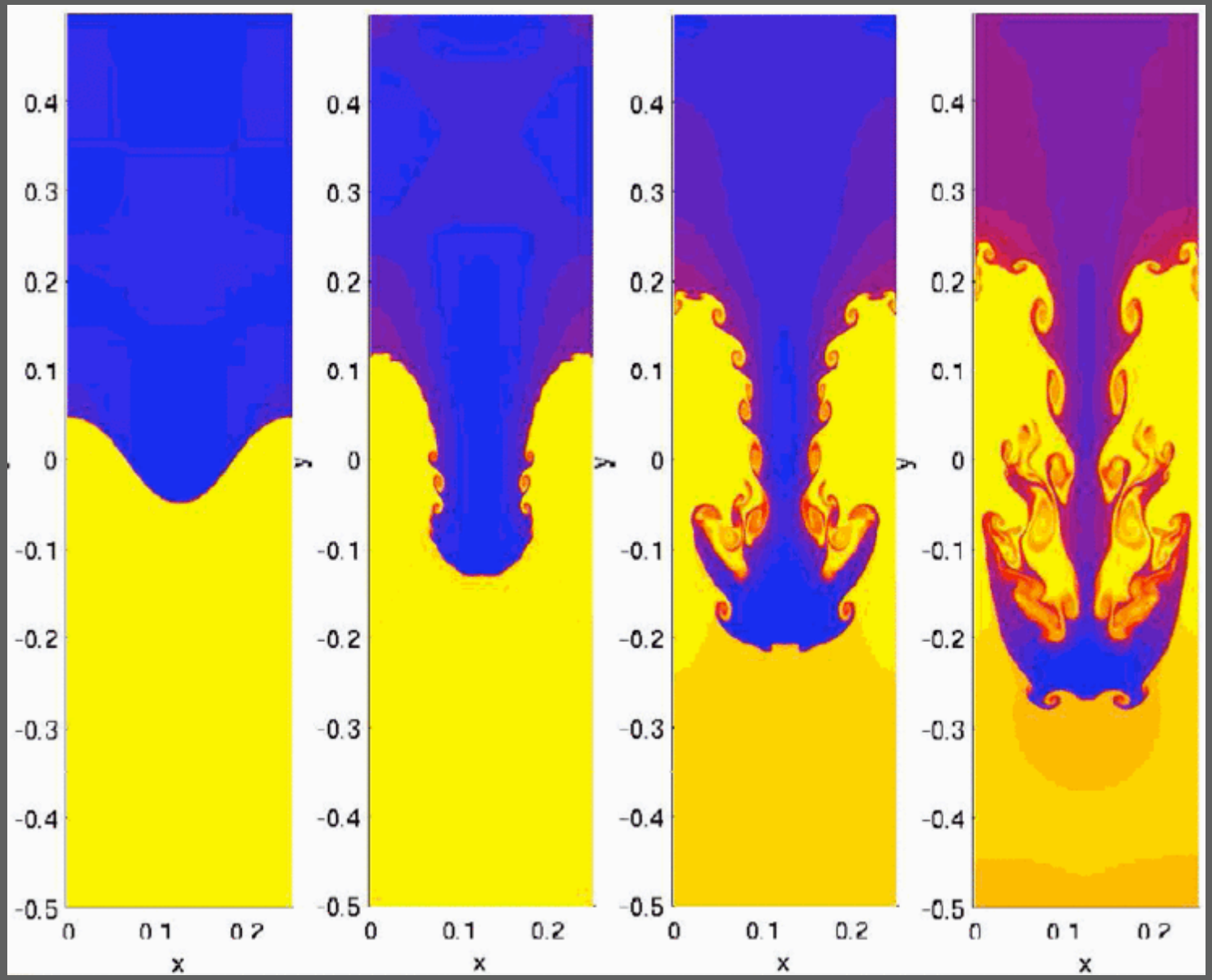

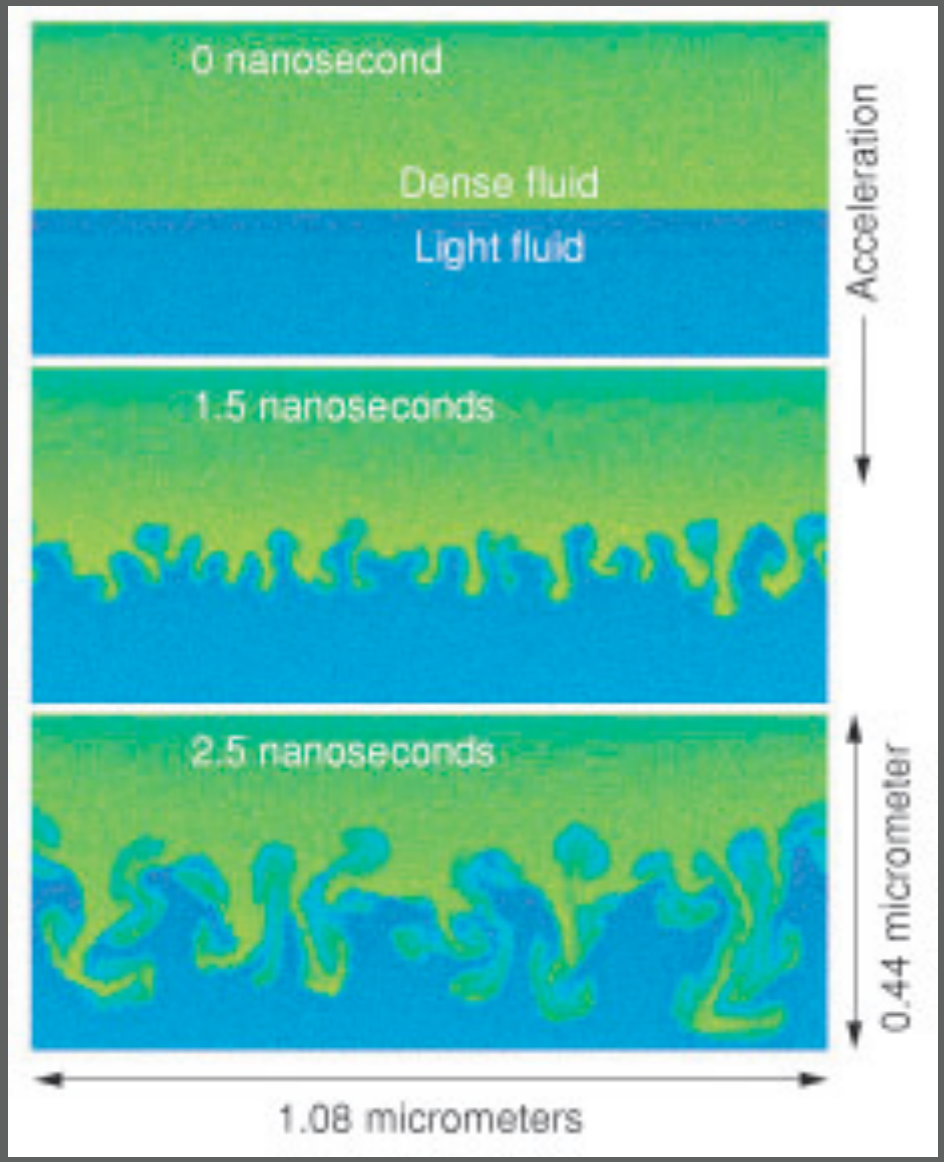
0 nanosecond
Dense fluid
Light fluid
Acceleration
1.5 nanoseconds
2.5 nanoseconds
0.44 micrometer
1.08 micrometers

Kelvin-Helmholtz instability

turbulence driven by large shear velocities

Richtmeyer-Meshkov instability

refracting waves crossing deformed interface

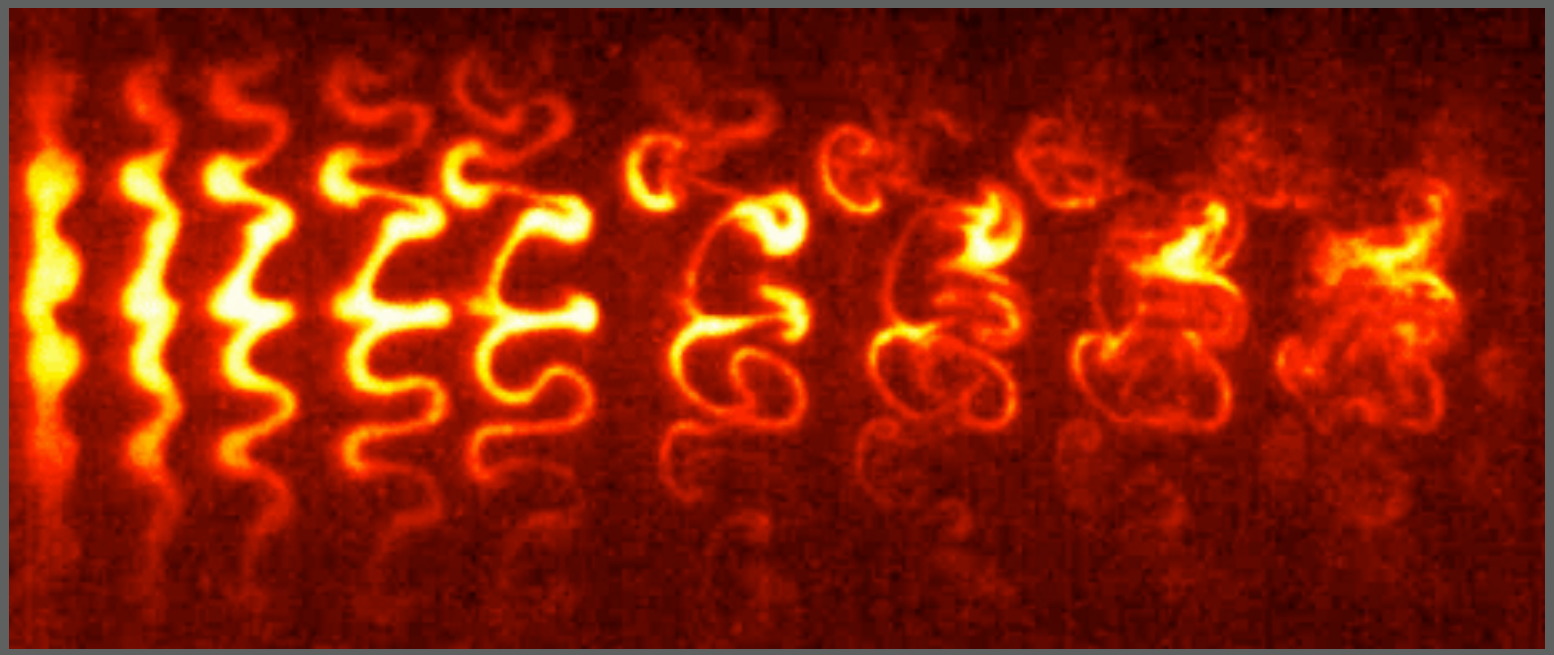

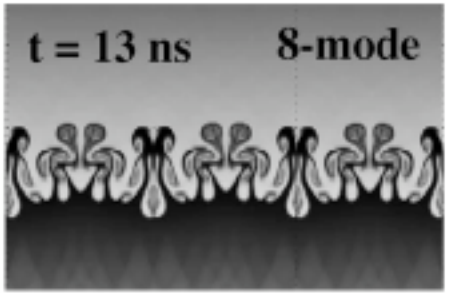

(a) **Numerical radiograph**

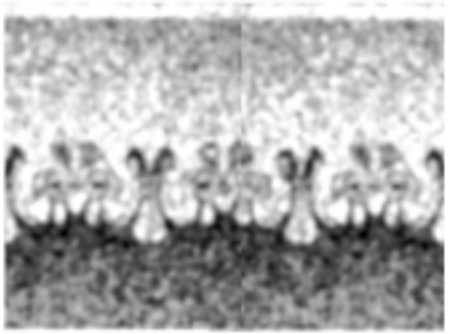

(b) **Simulated radiograph**

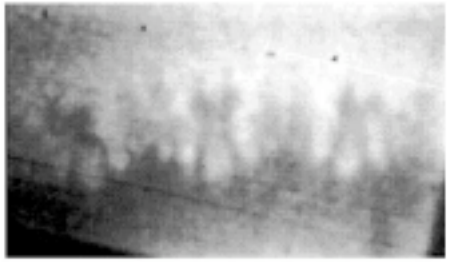

(c) **Experimental radiograph**

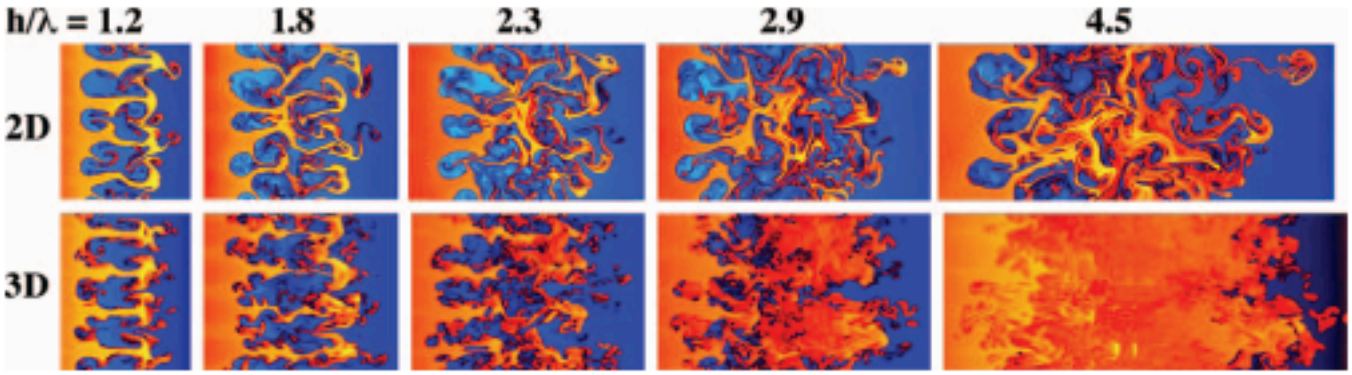

FIG. 13. (Color) Results from adaptive mesh refinement simulations of a proposed scaled SN hydrodynamics experiment for NIF. The hypothetical experiment simulated was assumed to be similar to that described in Fig. 12, except that it was driven harder, with a $M \sim 20$ shock. Also, a 3D high mode number noise spectrum was added onto the 2D single-mode perturbation as a seed. The top row was for simulations run in 2D, versus the bottom row was done in 3D with an adaptive mesh refinement code. With simulations run in 3D, with a 3D high-frequency noise spectrum, the deep nonlinear RT evolution is observed computationally to pass through the mixing transition, and enter a fully turbulent regime. Adapted from Miles *et al.*, 2005.

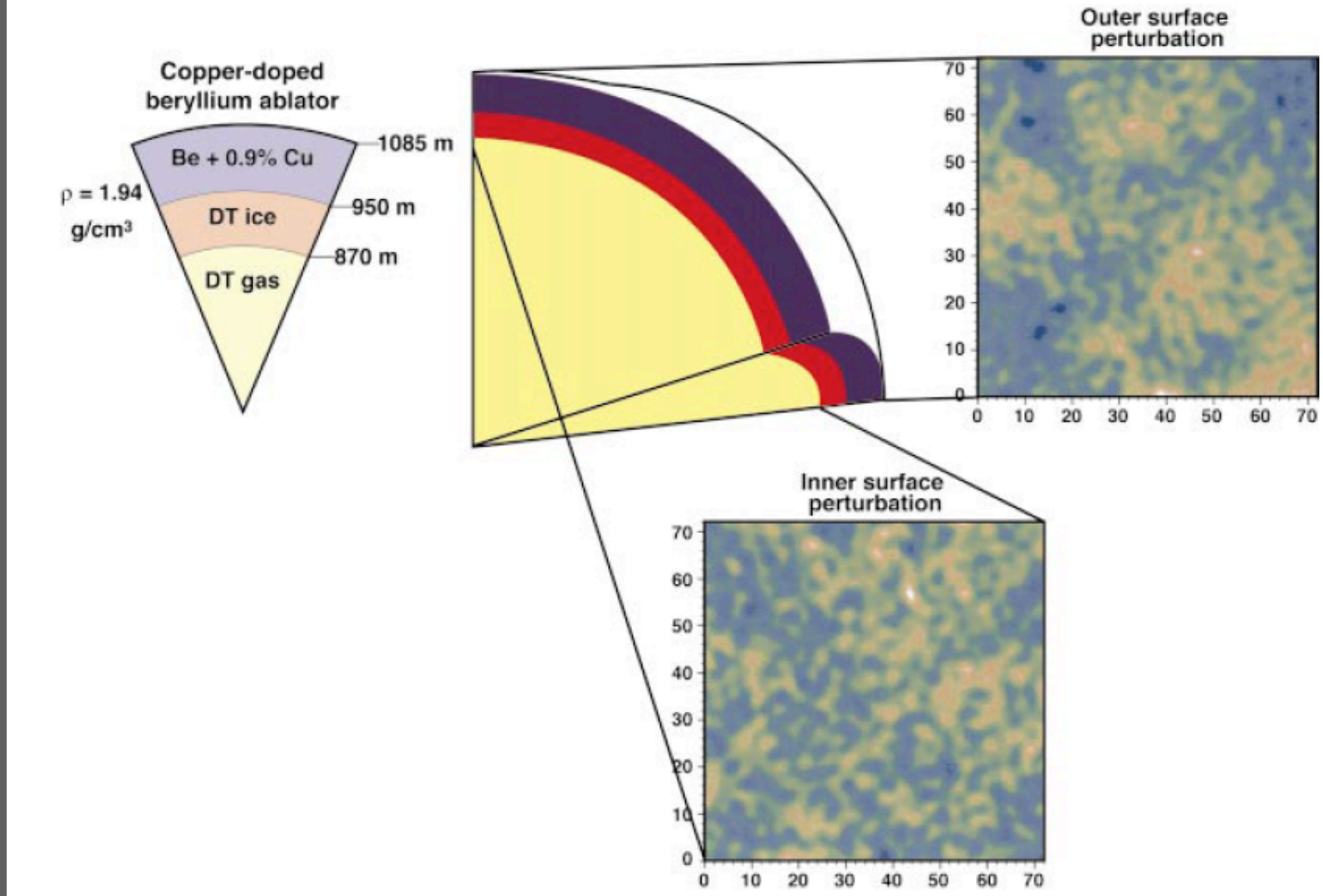

FIG. 2-8. (Color) Capsule-only simulations in 3D examine the effect of multimode surface perturbations. Both the inner ice and outer ablator surfaces are perturbed with modes over the range responsible for mix. Perturbations shown are derived from measured spectra of DT ice and a Nova capsule ablator, respectively.

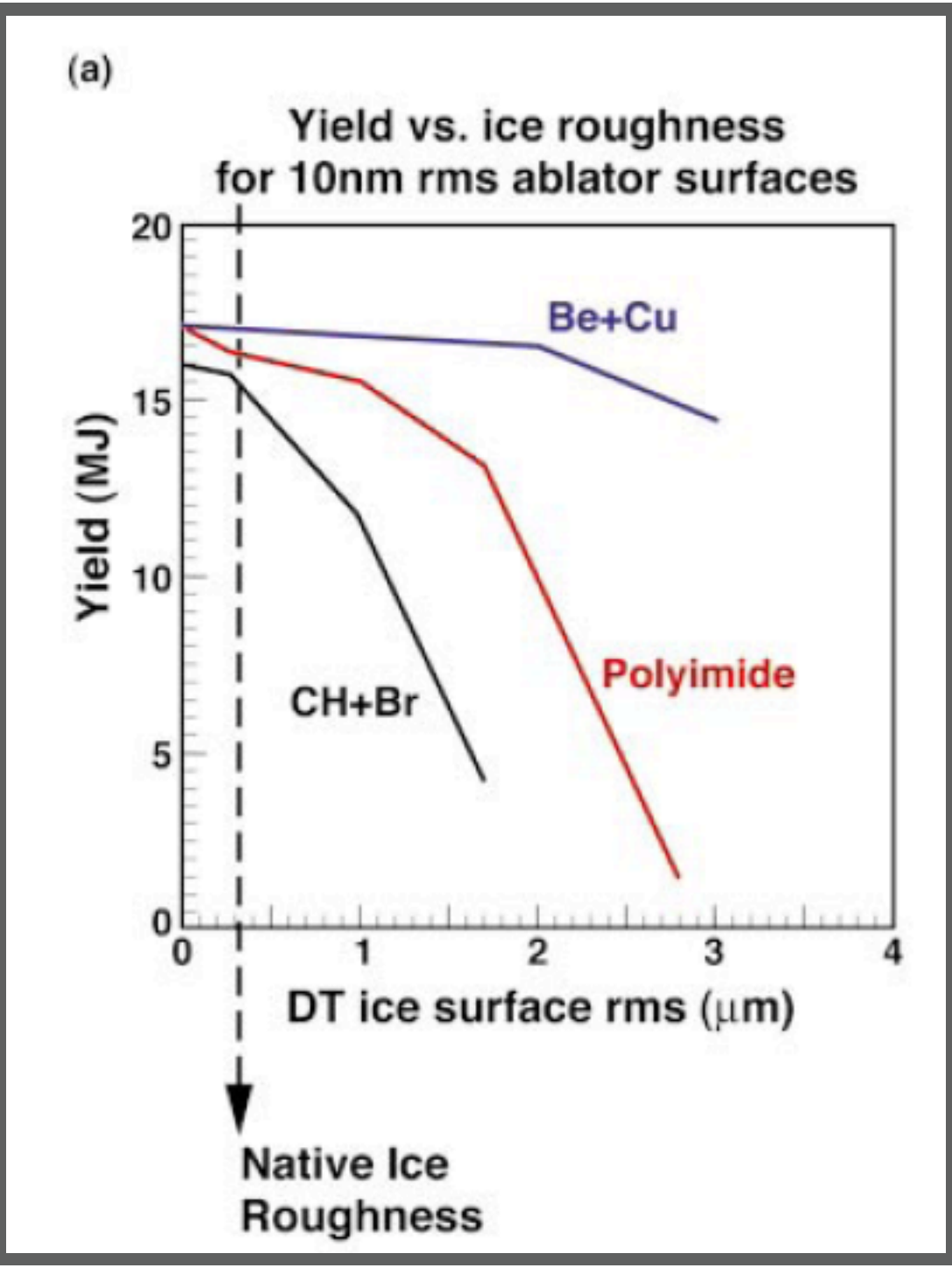
(a)
Yield vs. ice roughness
for 10nm rms ablator surfaces
Yield (MJ)
20
15
10
5
0
0
1
2
3
4
DT ice surface rms (μm)
Be+Cu
Polyimide
CH+Br
Native Ice
Roughness

Astrophysical data

Experimental data

Numerical simulations

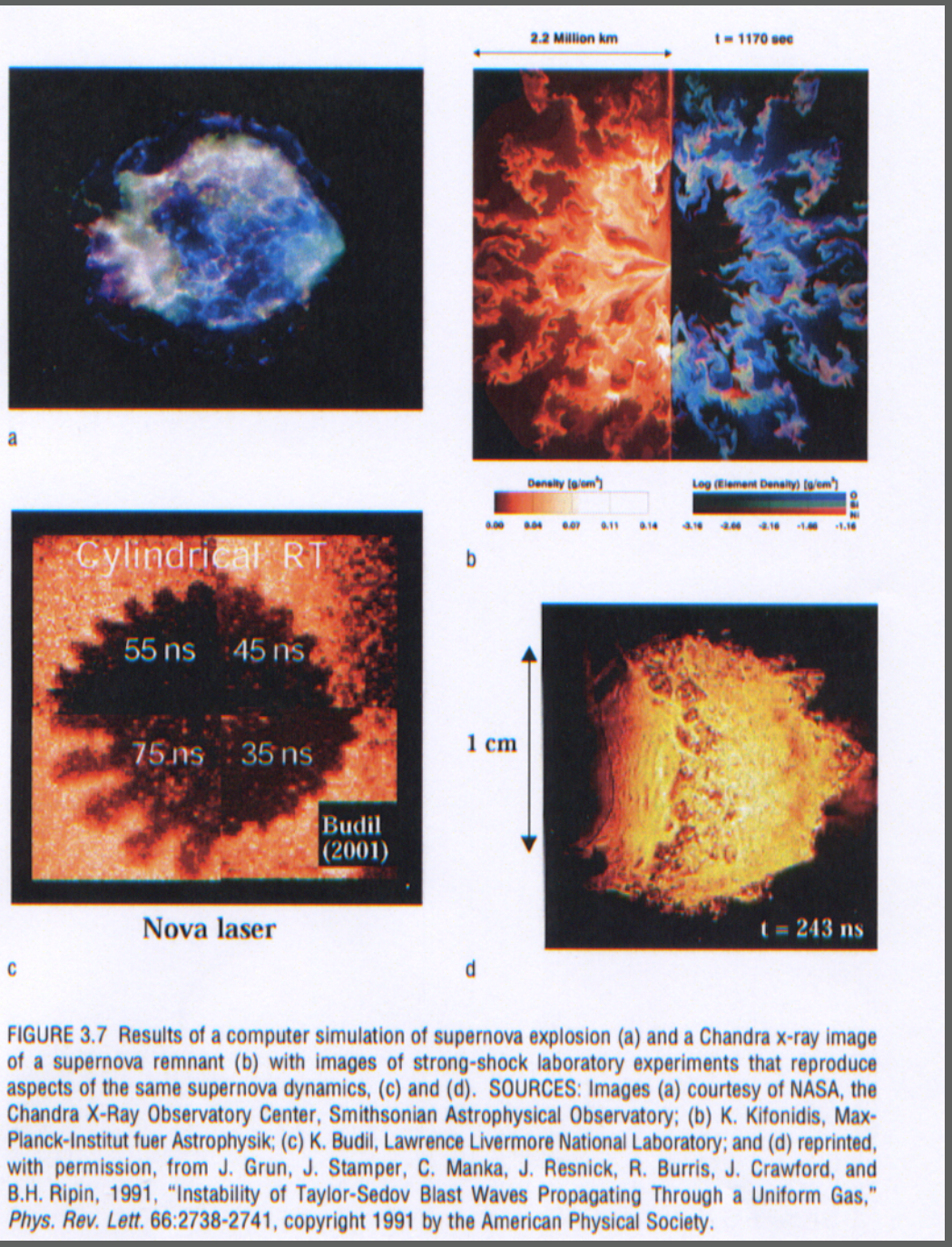

FIGURE 3.7 Results of a computer simulation of supernova explosion (a) and a Chandra x-ray image of a supernova remnant (b) with images of strong-shock laboratory experiments that reproduce aspects of the same supernova dynamics, (c) and (d). SOURCES: Images (a) courtesy of NASA, the Chandra X-Ray Observatory Center, Smithsonian Astrophysical Observatory; (b) K. Kifonidis, Max-Planck-Institut fuer Astrophysik; (c) K. Budil, Lawrence Livermore National Laboratory; and (d) reprinted, with permission, from J. Grun, J. Stamper, C. Manka, J. Resnick, R. Burris, J. Crawford, and B.H. Ripin, 1991, "Instability of Taylor-Sedov Blast Waves Propagating Through a Uniform Gas," *Phys. Rev. Lett.* 66:2738-2741, copyright 1991 by the American Physical Society.

Conclusions

NIF opens up a new regime of HEDP parameter space

Inertial Confinement Fusion, basic physics, (weapons), laboratory astrophysics

Gail Glendinning's talk is at 12:45 next Friday, October 31